Focal Coil Design for Transcranial Magnetic Stimulation on Mice

Bachelor graduation thesis
TU Delft - Electrical Engineering

Authors:

Jefferson Vegas, 4315979
Alexander Misdorp, 4240561

Supervised by:

Prof.dr.ir. Wouter Serdijn
Ing. Ali Kaichouhi

In collaboration with Erasmus MC:

Drs. Myrthe Ottenhoff
Dr. Bas Koekkoek

July 8, 2016

TU Delft Delft University of Technology

Erasmus MC

ABSTRACT

Background: Transcranial Magnetic Stimulation (TMS) is a non-invasive and painless tool that utilizes coil induced electric fields to stimulate certain areas of the brain. TMS on mice allows for the use of extra measuring tools normally not applicable to the human specimen, such that the consequences of TMS can be analyzed. Development of a coil suitable for TMS on mice is important as it offers rapid progress in this research field.
Objective: Design a TMS coil suited for focal stimulation on mice.
Methods: The electric field induced in a spherical mouse head model by seven different TMS coils are simulated with the finite element method. For each coil design, we quantified the electric field penetration at the brain depth where the electric field is half its maximum value ($d_{1/2}$), the brain volume where the electric field is half its maximum value ($V_{1/2}$), and the focality by the tangential spread defined as $S_{1/2} = \frac{V_{1/2}}{d_{1/2}}$. The influence of coil geometry parameters like wire thickness, inner coil radius, and number of turns on the focality are studied. Besides that, heating and force are taken into account based on calculations and simulations.
Results: The figure-8 and the overlap figure-8 coil prove to be the most focal coils that can reach $110\,\mathrm{V\,m^{-1}}$ with a focality of $49.62\,\mathrm{mm}^2$ and $43\,\mathrm{mm}^2$ respectively, lower than that of existing coils. Heat development indicates the need for active cooling while the exerted forces require epoxy to keep the coil in place.
Conclusion: A theoretical foundation has been set which paved the way for a practical realisation of a focal coil suitable for TMS on mice.

ACKNOWLEDGEMENTS

We wish to express our sincere gratitude to ing. Ali Kaichouhi for his guidance and encouragement in carrying out this project work.

Also, we are very thankful towards prof.dr.ir. Wouter Serdijn for supervising this project.

We would very much like to thank Mr. Ron van Puffelen for his help with the casing design and production.

Lastly, we would also really like to thank Drs. Myrthe Julia Ottenhoff & Dr. Bas Koekkoek for providing this project and giving us the necessary tools for its realization.

CONTENTS

1

PREFACE

This thesis is our final work as partial fulfillment for the Bachelor of Science in Electrical Engineering degree, at the TU Delft faculty of EEMCS and was conducted from April 2016 to June 2016 for eight weeks.

Working on this project for the past few weeks has been very intensive, educational and interesting as well. We got the opportunity to combine knowledge acquired during our bachelor together with neuroscience, which was a totally new and challenging field for us. It was also the final step towards a completed bachelor which was an extra encouragement to do better.

We were also encouraged to work outside our comfort zone and look at ethical issues in engineering design. This is especially applicable to our case because the system we developed is meant for research on animals, which is a big ethical concern in our society. Furthermore, we expanded our research and looked at the marketability of potential applications of this technology. These parts however, are not discussed in this report but will be presented in a business pitch at the final symposium.

Altogether we thoroughly enjoyed the experience of acting like a small business and developing our own product. It was a nice way to apply the accumulated knowledge throughout the past few years into a practical design. We hope our final product will comply to the standards set by the TU Delft and Erasmus MC and can contribute to research on Transcranial Magnetic Stimulation.

2

INTRODUCTION

Nowadays, in a world of increasing life expectancy, human kind has been on a slow but steady transition from a predominantly youthful population to an older one. As no transition happens without any implications, the number of neurological disorders has also increased. A lot of research is done on these conditions for the sake of earlier diagnosis and better treatment methods. However, most of these studies are done using invasive techniques or other techniques that are not yet as effective as we would like them to be. Transcranial Magnetic Stimulation may offer a novel solution to the problems regarding neurological disorders.

Transcranial Magnetic Stimulation (TMS) is a relatively new and non-invasive tool used by researchers for electrical stimulation of certain brain regions, mainly different areas of the cerebral cortex [1]. This technique is based on the principle of electromagnetic induction, whereby an electric field is produced due to time varying magnetic field generated inside the brain. The induced electric field, in turn, generates an electric current that modulates neurological activity.

As with any new medical tool we ought to ask ourselves what these new techniques have to offer that established methods do not offer for prognostic, diagnostic and therapeutic applications in clinical neurology. TMS is currently FDA approved for treatment of migraine and depression [2] [3]. Researchers think TMS can also be used to explore various neural processes and treat a larger variety of neuropsychiatric illnesses [4] [5]. However, the specific underlying mechanism by which one can activate neurons is still unknown [6]. More research on TMS is needed for both improvement of the stimulating device, mostly the behavior of the coil, as well as for a systematic approach for using results acquired through TMS for proper diagnosis and better treatment methods. The development of systems suitable for TMS on mice are important as this offers rapid progress in this research field. This is because TMS on mice could be combined with more invasive methods for measurement of neuronal activity, which is not applicable on the human specimen.

Existing TMS coils are not suitable for use on mice as they are limited by non-focal electric field profiles and depth of stimulation due to a trade-off between these two factors. Current coils can thus either be used for the stimulation of quite large areas deep inside the brain or relatively small regions on the brain cortex. The figure-8 coil geometry is known for its relatively small stimulating focal point.

The focus of this project is to design a focal coil appropriate for mice such that research on potential medical benefits associated with TMS can be conducted. By simulating different coil configurations, the magnetic and electric field distributions inside the brain for each of these coils are studied. The different coils are then compared on aspects such as electric field strength and their focal point to find the one that is most suitable for this application.

In part one, background information to the subject of neuroscience, electromagnetic induction and TMS is given, which should provide the necessary basis in order to understand concepts concerning this technique and the development of the coil. Also, a state of the art analysis is given.

Part two starts off with the system requirements. Furthermore we describe the implementation of the coil using COMSOL Multiphysics Modeling Software 5.2, which is a finite element method (FEM) solver and simulation software package for various physics and engineering applications where different physic phenomena are coupled. The focus will be on the simulation of the electric and magnetic field distribution to be able to quantify the performance of different coils for comparison with each other. Besides that, heat development and exerted forces are studied. We conclude this part by describing the final coil design and reflect on whether this design meets the requirements.

Part three documents the strategy that will be used to test the coil in practice.

Lastly, the thesis will be completed by an overall conclusion.

3

PROJECT DESCRIPTION

3.1 PROBLEM DEFINITION

TMS has been in use for at least three decades but the operating principles behind this technique are still widely unknown. Invasive extra-cellular recordings are necessary to gain a deeper understanding. This could potentially lead to a better and more reliable application of this technique. These recordings however can not be performed on the human specimen and need to be performed on animals like mice. Mice however, have significantly smaller brains and thus require more focal stimulation. To accomplish this, smaller coils are necessary. Because stimulation requires large coil currents, heating issues arise. An optimum has to be found between focal stimulation and a coil that does not overheat. This leads to the following problem statement:

Can we develop a coil suitable for TMS on mice?

3.2 PROPOSED SOLUTION

The complete system consists of software, hardware and the coil. Each of these sub-parts are subsequently divided among our team. We are devoted to coil design. Designing the coil requires study of magnetic and electric fields, heat development, interactive forces and the skin effect inside the wire. Apart of that a casing has to be designed. With the use of COMSOL Multiphysics, a FEM analysis tool, the magnetic and electric field will be modelled to get an understanding of their distributions inside the head. This way we can vary the coil's geometry characteristics and observe its influence. Heat development and interactive forces are two other quantities that will be calculated or modelled with COMSOL Multiphysics. This will allow us to determine whether active cooling is necessary to prevent overheating. We may also conclude measures are necessary to ensure the coil does not break under its own force. The skin effect, the tendency of AC current to flow unevenly inside a conductor such that the current density is larger near the surface of the conductor, can be studied by applying the Fourier Transform on the applied pulse in MATLAB.

The skin effect might play part in heating, force and field distributions. Lastly, we will design a casing in CAD Tools with the help of Ron van Puffelen and 3D print it afterwards.

Following these steps we aim to design a focal coil exempt from heating issues, capable of stimulating a mouse brain.

Part I

THEORY

4

THEORETICAL FRAMEWORK

4.1 NEUROSCIENCE

Neuroscience is a research field concerned with the workings of the nervous system and impact on behavioral and cognitive functions. The nervous system is comprised of a large set of neurons that allows communication between different parts of the body [7]. The human brain alone contains about 86 billions neurons [8]. As seen in figure 2, a single neuron consists of a cell body, dendrites, and an axon. The cell body contains the nucleus that is necessary for cellular function. Dendrites are responsible for receiving signals while an axon transmits signals.

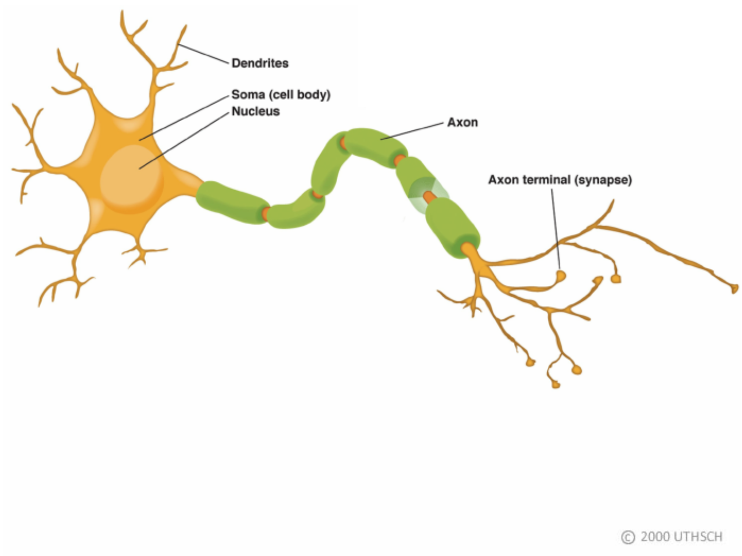

Figure 2.: *A neuron consists of a nucleus, an axon, and dendrites [9].*

Interconnected neurons can relay signals over a minuscule gap between a dendrite and axon known as the synapse. Signal generation occurs whenever a neuron is properly stimulated. TMS allows for such stimuli, due to the creation of an electric field inside the brain. Stimulation causes an electric current to flow down the axon towards the synapse. Molecules known as neurotransmitters cross the gap to relay signals from one neuron to an other.

The inner and outside of a neuron are separated by a cell membrane as represented in figure 2 by the green layer. Due to different ion concentrations a potential difference of -70 mV on the inside with respect to the outside over the membrane is registered. This potential difference is called the resting potential and can be disturbed by a stimulus to trigger an action potential that travels down the axon. Figure 3 shows that in case a stimulus manages to reach the -55 mV threshold, depolarization occurs. This irreversible process causes the voltage to reach up to 40 mV whereafter it repolarizes back to the resting potential. For a small period in time hyperpolarization occurs, the voltage will drop below -70 mV during which no other action potentials can be generated while the potential increases back to the resting potential [9].

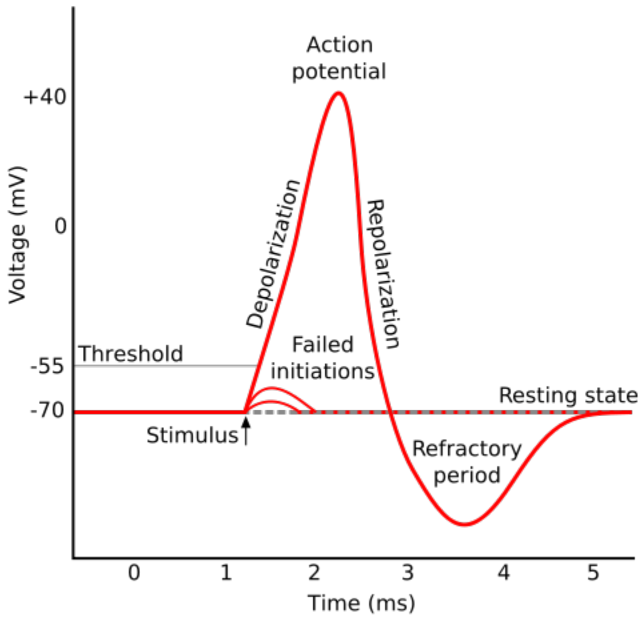

Figure 3.: *After a couple of failed initiations the threshold is reached which causes an action potential to be generated. Before returning to rest potential, hyperpolarization occurs [9].*

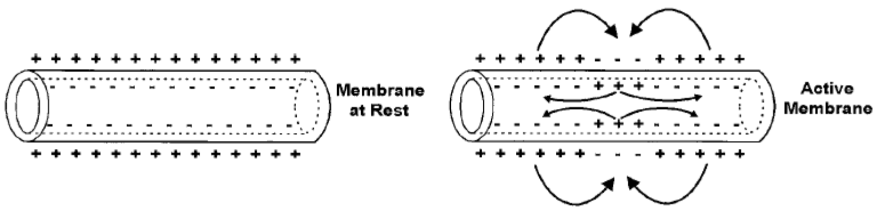

Figure 4.: *The membrane voltage is stimulated which leads to an action potential that subsequently travels down the axon of a neuron [10].*

4.2 ELECTROMAGNETIC INDUCTION

The fundamentals of TMS are based on the principle of electromagnetic induction. Faraday's law, as stated in equation 1, implies that an electric field (E) is induced in a closed circuit, equal to the negative of the time rate of change of the magnetic field (B) enclosed by this circuit.

$$\nabla \times E = -\frac{\partial B}{\partial t} \tag{1}$$

In the case of TMS, the closed circuit is brain tissue whereby the currents induced are called eddy currents. These currents are in the same direction as the induced voltage. Lenz's law in equation 2 states that the direction of the induced voltage (ε), and thus the eddy current is in such a way as to oppose the varying magnetic flux (Φ).

$$\varepsilon = -\frac{\partial \Phi}{\partial t} \tag{2}$$

Following the Biot-Savart law seen in equation 3, an electric current (I) generates a magnetic field [11].

$$d\mathbf{B} = \frac{\mu_0}{4\pi}\frac{Id\ell \times \hat{\mathbf{r}}}{r^2} \tag{3}$$

It's important to note that the magnetic field distribution is only reliant on the current path ($d\ell$). According to Ampere's law, a closed contour (Amperian loop) should be drawn around the current source as seen in figure 5. In accordance with equation 4 this means that the magnetic field is only reliant on the current enclosed by the Amperian loop. Therefore only the amount of current through the Amperian loop and not the wire characteristics are relevant for determining the magnetic field [12].

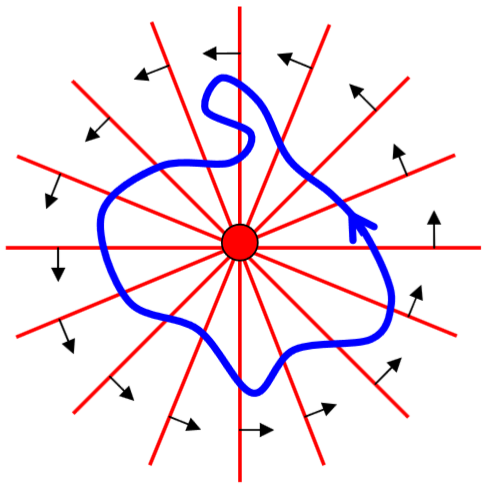

Figure 5.: *The blue contour indicates the Amperian loop around the red current carying wire. The black arrows indicate the direction of the magnetic field [13].*

$$\oint_C B \cdot d\ell = \mu_0 I_C \tag{4}$$

By combining these laws it can be seen that a coil with sufficient varying electric current passed through it, placed above the head of a mouse, causes an electric field inside the brain.

The quasistatic domain is concerned with systems that are small compared to the electromagnetic wavelength. As we will see in Section 7.2, the highest frequency component in the current signal is approximately 10 kHz. The associated wavelength is 30 km and thus significantly bigger than the coil dimensions. Under quasistatic conditions EM fields can be considered as being static. This allows for the use of simpler static field equations like the Biot-Savart law.
Retarded time is left out of consideration because it's assumed that the EM field at a short distance of the coil instantaneously changes with the EM field at the coil [14] [15].

4.3 TRANSCRANIAL MAGNETIC STIMULATION

The field of electrophysiology, which studies the electrical properties of biological tissue, was born in 1771 with the discovery of bioelectricity by the Italian physician Luigi Galvani. Since then, several tools have been developed to exploit this technique, culminating into the first reliable and non-invasive brain stimulator developed by Anthony Barker in 1985 [3].

Unlike Transcranial Electrical Stimulation (TES) and Deep brain stimulation (DBS), TMS is a rather safe and painless method to study the integrity of the brain. This technique is used in diagnostics to evaluate damage from injuries and other disorders as well as treatment of these injuries and brain mapping [6].

4.3.1 *Stimulation*

With TMS, strong magnetic pulses penetrate through scalp and skull to reach the brain without significant attenuation. These pulses generate secondary currents inside the brain that modulate neuronal activity. The induced electric field causes ions to flow in the brain without the need for current to flow across the skull, and without charged particles being injected into the scalp [16].

The ability of TMS to depolarize neurons depends on the activating function, which causes transmembrane current to flow and can be described mathematically by the spatial derivative of the electric field along a nerve [1]. As a result, the point of stimulation will be at the point along the nerve where the spatial derivative of the electric field is maximum. The situation is a bit different for bent nerves. Here, nerves bend across the induced electric field so that the induced currents flow through the membrane, causing bent nerves to be preferential points of stimulation. This principle is illustrated in figure 6.

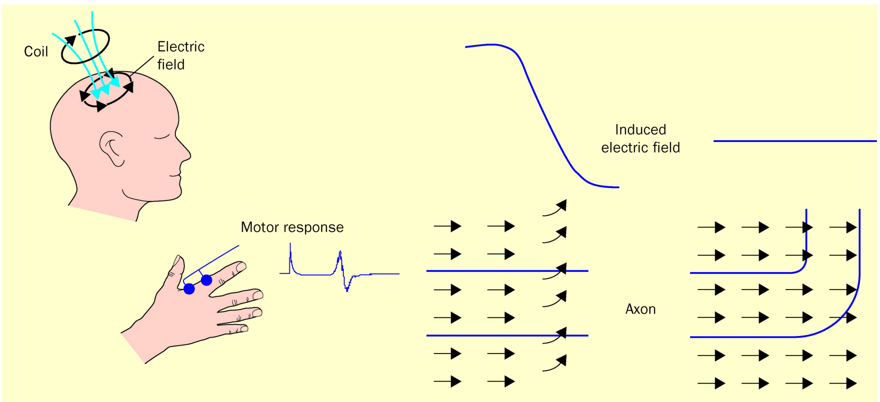

Figure 6.: *"Principle of TMS. Left: the current flowing briefly in the coil generates a changing magnetic field that induces an electric current in the tissue, in the opposite direction. Middle: schematic illustration of the current flow due to the induced electric field that changes along the length of a nerve fibre and results in a transmembrane current. Right: a bent nerve and the uniform current in the uniform electric field also results in a transmembrane current" [1].*

4.3.2 *TMS protocols*

Multiple TMS protocols have been developed which show specific advantages for different applications of this technique. The effects of TMS can be divided into three types depending on the used protocol for stimulation.

4.3.2.1 *Single Pulse TMS*

The single-pulse TMS protocol is used for depolarization of neurons in de neocortex to unload an action potential. A single current burst is released into the stimulating coil to stimulate neurons only once. If the stimulating neurons lie in the motoric cortex, muscle activity is produced, which is referred to as motor evoked potential (MEP). MEP intensities vary depending on the strength of the stimulating electric field.

4.3.2.2 *Paired-Pulse TMS*

In paired-pulse TMS, two different current pulses, are sent through the coil, each with different intensities and varying time intervals ($1-20\,\mathrm{ms}$) also known as the interstimulus interval (ISI). This technique can be used to study dynamical aspects of neuroactivity.
For example, inhibitory and facilitatory interactions in the cortex can be studied by combining a subthreshold conditioning stimulus with a suprathreshold test stimulus at different short interstimulus intervals through the same TMS coil [1].

4.3.2.3 *Repetitive TMS (rTMS)*

The first two protocols were most used a few decades ago. However, due to advancements in the development of magnetic stimulation devices, rTMS has become possible and is currently the most common technique [17]. rTMS consists of a train of stimulating pulses (1-20 pulses per second), all with the same intensity. rTMS can produce long lasting effects that are not only limited to the period of stimulation. Most of these effects are related to the excitability of the treated areas and are highly dependent on stimulus frequency and intensity. However, the exact mechanisms behind these effects is still not clear.

Present TMS devices can produce two different stimulus waveforms, where the induced current is either monophasic or biphasic.
Studies done with single pulse TMS show biphasic pulse are more effective for stimulation in the sense that they are more powerful than monophasic waveforms [18].

4.3.2.4 *Adverse Effects*

Although TMS is generally regarded as safe, there are still a few potential side effects associated with this technique. These side effects are more common in high frequency rTMS. The most obvious and dangerous side effect of rTMS is the provocation of epileptic seizures and experience shows that currently available equipment is powerful enough to produce these [16].

Different studies suggest that even at dangerous TMS intensities and long treatment durations, there is a very small possibility of structural brain damage [19]. More research needs to be conducted to see if there are any possible long-term side effects, however for now, there is no indication that this is the case.

5

STATE OF THE ART COIL DESIGN FOR TMS

Because TMS has been in development since the 80's, a lot of research has been conducted on this concept. This ranges from the possible treatment of various illness, to the electrophysiological workings, but also the design of coils. Back in 1985, Anthony Barker and colleagues developed the first coil suitable for TMS on the human specimen [20][21] as seen in figure 7. This involved a circular coil capable of nerve stimulation. These coils stimulate a rather large area though as the magnitude of the induced eddy current is the same everywhere. The need for more focal stimulation lead to the development of new coil designs, with the figure-8 coil being the most prominent. As the name implies, the coil is shaped like a figure 8 and is shown in figure 8a.

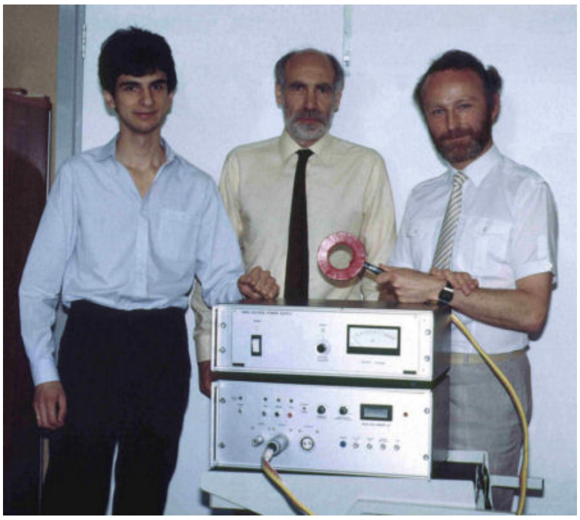

Figure 7.: *Anthony Barker and his colleagues proudly show their circular TMS coil.*

As the idea behind TMS is to induce eddy currents in the brain according to the physics described in Section 4.2, the idea behind the figure-8 coil is to add up two eddy currents in a small region of the brain. The net result is that the stimulation is twice as strong right under the area where the two circular coils touch, as compared to elsewhere underneath the circular coils. For optimal stimulation one also has to consider the right position and angle under which the coil is positioned above the head. The correct placement is shown in figure 8b, two

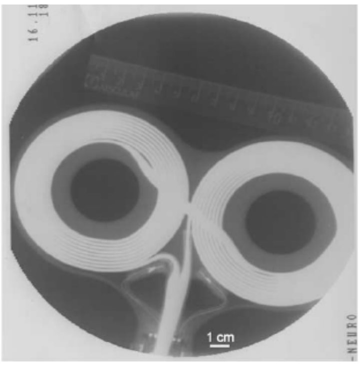

(a) *X-ray of a Magstim Coil [22].*

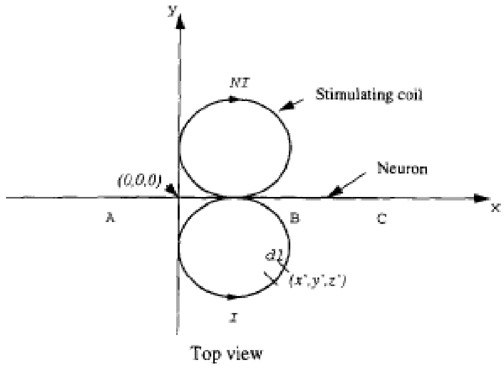

(b) *Positioning of a figure-8 coil above a neuron for excitation [23].*

Figure 8.: *Figure-8 coil*

Because of its focality and ability to create strong magnetic fields, the figure-8 coil is the most popular and commercially available TMS coil. Besides the circular coil, almost no other TMS coils are sold. For the more specific application of Deep TMS whereby stimulation occurs deeper into the brain, so called H-coils are available. These however, are not of interest to us because our stimulation point is not considered deep with just a 5 mm distance from the coil.

A lot of other coil designs have mainly been considered in theory and simulation. Zhi-De Deng et al. considered 50 different coil designs, figure 9 shows some of these coils [24]. From the research they have conducted it became clear that the figure-8 based coils have the highest focality. For this reason we decided to base our simulations on the figure-8 geometry.

(a) *Slinky figure-8 coil*

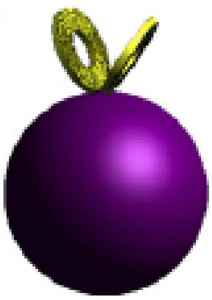

(b) *V-coil, a bend figure-8 coil*

(c) *Circular coil with multiple layers*

Figure 9.: *A grasp of the simulated coil geometries by Zhi-Deng et al. [22].*

An important distinction between these existing coils and the coil we are ought to design is the scale. Existing TMS coils are designed for the human specimen or on rare occasion for rats [25]. A mouse brain is a lot smaller than a human brain and weighs only 0.4 g whereas a human brain weighs about 1320 g [26]. Even though the required electric and magnetic field strengths are approximately the same, the stimulation area is a lot smaller. This requires much smaller coils as that reduces the stimulation area. Some problems arise from this requirement, the first concern is about the feasibility of the required focality. Secondly, smaller wires lead to higher resistances. And because heating can already be a concern for human specific TMS coils, it could become even more of an issue. Thirdly, forces come into play and one has to oversee that the coil does not succumb under its own forces.

TMS coils suited for mice are therefore nearly non-existent, we found only one design that was created by Iowa State University [27]. However, their settings differs from ours as they required the mouse to wear a helmet.
Besides that, there was a different focality requirement as their ideal focality was 115 mm^2, much higher than we aspire. The design consisted of two circular, so called "halo coils", whereby the mouse head is placed into one of the coils, and the other coil is placed on top of the head as seen in figure 10.

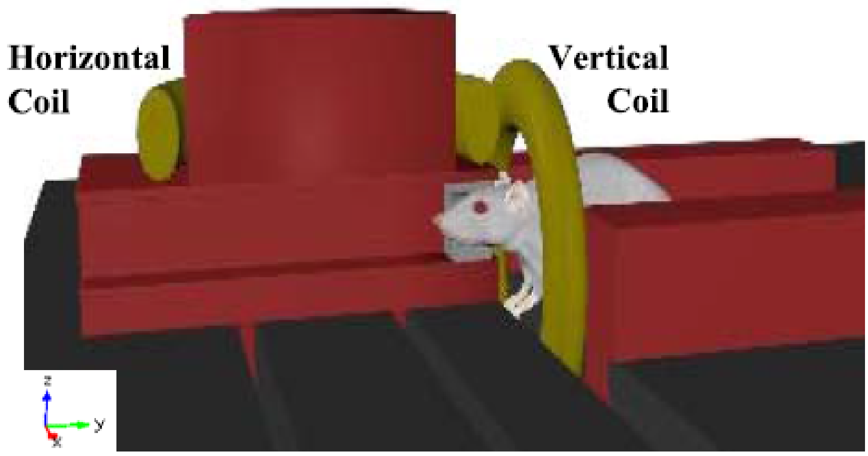

Figure 10.: *Iowa State University coil design that includes a helmet (red) and two circular coils (gold).*

Part II

DESIGN

6

SYSTEM REQUIREMENTS

The coil is the only part of the system that is near the mouse during stimulation of the brain. Hereby, it is subjected to functional requirements as well as safety requirements which guarantee a safe environment for the mouse and user. In this chapter a description of the coil specifications is given according to which the coil will be designed. The coil specifications are shown in table 1 below.

Table 1.: *Coil specifications*

Nr.	Requirement	Requirement/Wish
1	All system components in contact with the user and patient should be electrically isolated	Requirement
2	The coil should have a suitable casing	Requirement
3	The coil should be able to handle paired pulses with interstimilus interval (ISI) of 3 ms	Requirement
4	The coil should be able to handle paired pulses with an interstimulus interval (ISI) programmable between 1.5 ms and 3 ms	Wish
5	The coil should be able to handle a paired pulse followed by another paired pulse five seconds later repetitively for 200 times.	Requirement
6	The casing should be kept at a temperature lower than 41 °C at the surface in contact with the mouse head	Requirement
7	The induced electric field 5 mm deep inside the head should be at least $110\,\mathrm{V\,m^{-1}}$	Requirement
8	The electric field should stimulate a maximum area of 1 mm x 1 mm	Requirement
9	The electric field should stimulate a maximum area of 0.5 mm x 0.5 mm	Wish
10	The designed coil must be a figure-8 coil	Requirement
11	Alternative coil geometries derived from the figure-8 coil may be designed as well	Wish

As specified by requirement 7, an electric field of $110\,\mathrm{V\,m^{-1}}$ should be induced 5 mm deep inside the head. We did our own research on this requirement and discussed it with the supervisors as it was not specified upfront. This value was based on different studies [28] [29]. Lower electric field intensities can be controlled by varying the current through the coil, this is regulated by the hardware [30] and software [31].
The stimulus area, as specified in requirement 8 and 9 defines a square area to be stimulated. However, an absolute specification on how this area should be calculated is loosely defined. For our comparisons we shall use the definition described in Section 7.1 to give us a standardized way for comparison. This definition however can not be directly compared to the stimulation area set in these requirements. It allows us to quantify focality and compare it with existing TMS coils. Improvement on this parameter would therefore indicate improved focality compared to existing TMS coils.

7

FIELD SIMULATIONS

In this chapter, the influence of coil parameters like number of turns, wire thickness and coil diameter on focality and intensity of the induced electric field are studied. Afterwards, seven different coil geometries are simulated and their performance parameters are compared in order to decide which one is the most suited for TMS on mice.

7.1 SIMULATION METHODS

The TMS coil and mouse head model were implemented with COMSOL Multiphysics Modeling Software 5.2. Because of the intended coil casing, the mouse head was placed 2 mm away from the coil and was modeled by a homogeneous sphere with a 1 cm radius and electrical conductivity of $0.33\,\mathrm{S\,m^{-1}}$ [24]. The mouse brain was modelled as a sphere with a 0.5 cm radius placed at the center of the head and with the same conductivity. The simulation setup is depicted in figure 11 for the case of a figure-8 coil. The distinct head tissue layers (scalp, skull, corticospinal fluid, and brain) were not differentiated, since magnetically induced electric field in a sphere is insensitive to radial variations of conductivity[32].

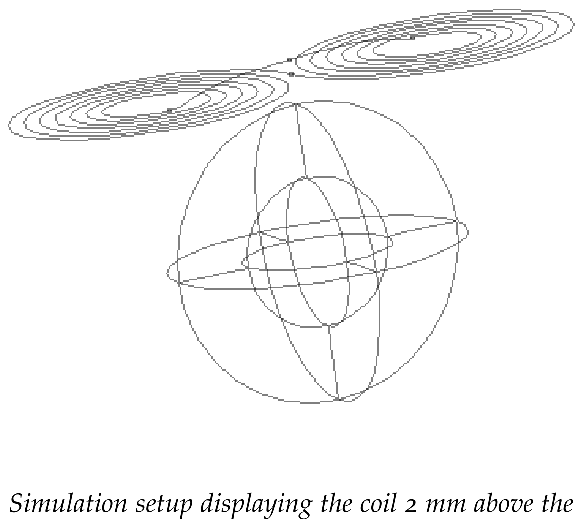

Figure 11.: *Simulation setup displaying the coil 2 mm above the head model.*

Coil geometries were drawn as current carrying line elements to analyze the electric and magnetic field distributions inside the head model. These line elements represent the current path and do not take wire thickness into account. This however has negligible influence on the magnetic and electric field distributions, as explained in section 4.2, which is why we approximate realistic wires by these line elements. To analyze the influence of wire thickness, we will vary the distance between the inner and outer radius of the coil assuming the wires are tightly wound together. Figure 12 illustrates this idea.

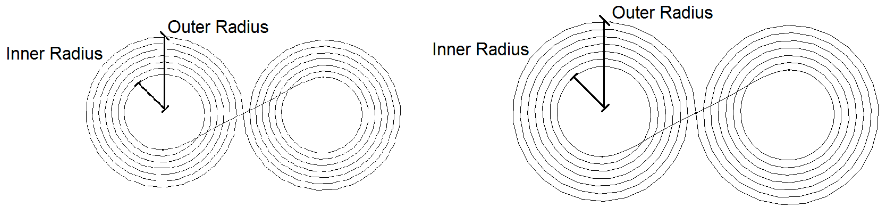

Figure 12.: *Left: Figure-8 coil of seven turns with inner radius of 3mm and outer radius of 10 mm, indicating a wire thickness of 1 mm.*
Right: Figure-8 coil of seven turns with inner radius of 3 mm and outer radius of 13.5 mm, indicating a wire thickness of 1.5 mm.

For each coil geometry, we measured the maximum electric field E_{max} at the brain surface. This value was used to calculate the half-value volume $V_{1/2}$, which is the volume of the brain exposed to an electric field stronger or as strong as half the value of E_{max}. The half-value depth $d_{1/2}$ was also calculated, which is the radial distance from the brain surface to the deepest point where the electric field is stronger or as strong as the half value of E_{max}. It is important to note that the deepest point where the electric field is half the value of E_{max} does not necessary fall beneath the same radial line as E_{max}. These definitions are illustrated in figure 13. In the rest of this paper we will be referring to these parameters as performance parameters. All these parameters were calculated 10 µs into the current pulse described in section 7.2.

These parameters are used to define focality by the tangential spread as $S_{1/2} = \frac{V_{1/2}}{d_{1/2}}$ and it has units of area.
It is important to note here that this definition of focality is not the same as the 1 mm x 1 mm stimulation area set by the the requirements. This is due to the fact that little is known about the actual area of stimulation and the specific thresholds for stimulation of different brain regions. However, measuring focality as the tangential spread $S_{1/2}$ allows us to quantify electric field hotspots inside the brain so that different coil geometries can be compared in terms of focality.

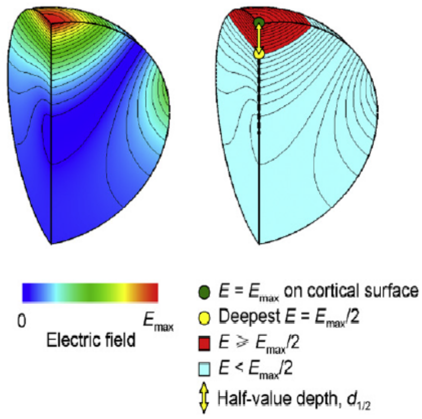

Figure 13.: *"Focality parameters are illustrated here. The left column shows the electric field strength contour and color map on the quarter-sphere segment of the brain. The right column shows the location of the maximum induced electric field on the brain surface, Emax (green circle), and the location of the deepest point where the electric field strength is the half value of E_{max} (yellow circle). The yellow arrow represents the half-value depth, $d_{1/2}$, which is the radial distance from the cortical surface to the deepest point where the electric field strength is half of its maximum value on the brain surface. The red portions of the quarter-sphere indicate the regions of the brain exposed to electric field as strong as or stronger than E_{max}; the total volume of these regions is $V_{1/2}$" [24].*

7.2 CURRENT PULSE ANALYSIS

The hardware team concerned with the system delivering the current pulse through the coil is aiming to deliver a current waveform as shown in figure 14. This waveform however represents the worst case scenario, as the duration might be shorter leading to less heating issues. It is a current waveform commonly used in TMS and will be used as the current through the coil in the simulation.

Important properties of this waveform are the small rise time of 70 µs up to 2500 A and the relatively large decreasing time until no current flows through the coil anymore. This current waveform gives a baseline for the required electric field intensity while the desired location is determined by the coil geometry. The frequency spectrum of this current waveform is shown in figure 15.

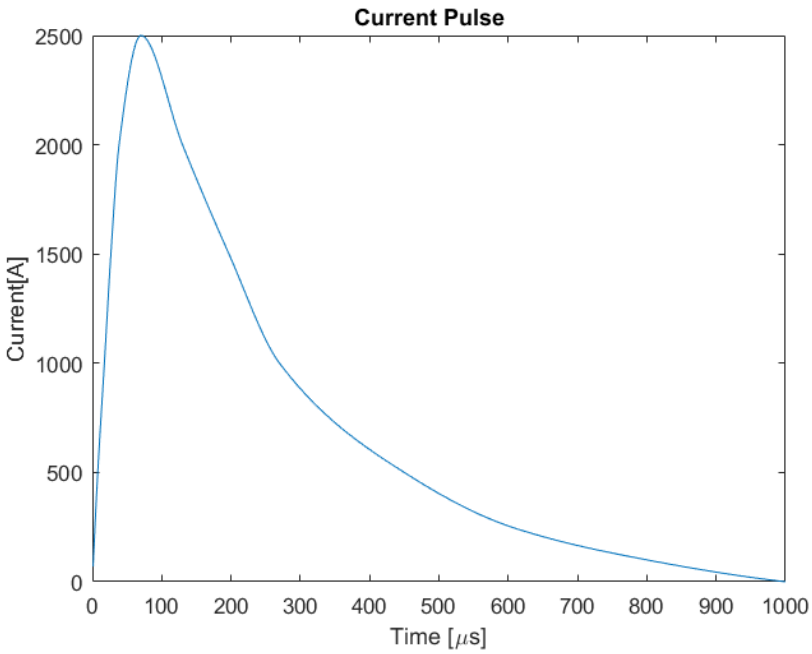

Figure 14.: *Current pulse waveform through wires used for simulation. This is a commonly used current waveform in TMS applications.*

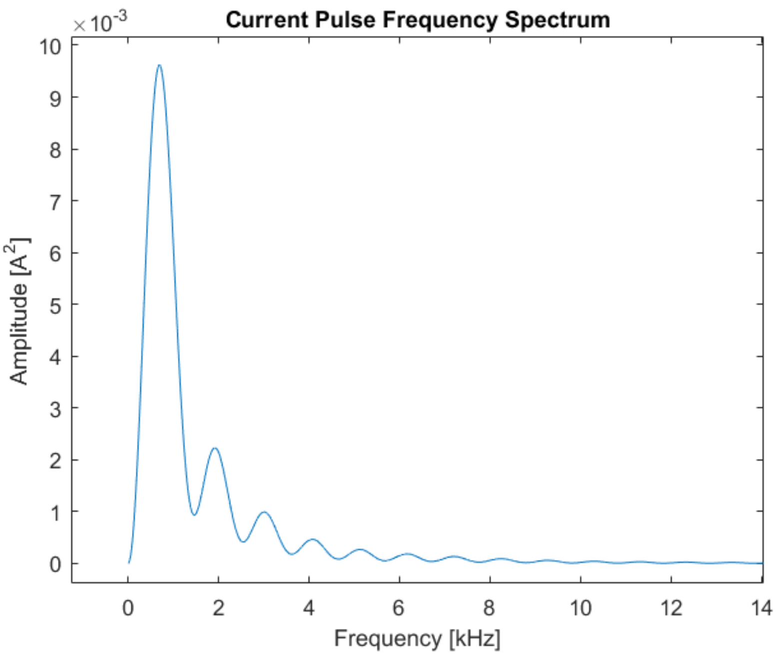

Figure 15.: *Frequency spectrum of the current waveform depicted in figure 14. The DC component of this signal was subtracted from the current pulse for better insight in low frequency components.*

7.3 SKIN EFFECT

As frequencies increase, the current inside a conductor begins to move from a homogeneous distribution through the conductor cross section towards current flow almost exclusively near the conductor surface. This phenomena is called the skin effect and is caused by circulating eddy currents reducing the current flow in the center of a conductor and enlarging it on the surface. Skin depth (δ) is a measure of the depth at which the current density falls to e^{-1} of its value near the surface and is calculated with equation 5,

$$\delta = \sqrt{\frac{\rho}{\pi \times f \times \mu}} \tag{5}$$

and is dependent on the resistivity of the conductor (ρ), the frequency (f) and the absolute magnetic permeability (μ) of the conductor. The skin depth for a copper conductor as a function of frequency is shown in figure 16.

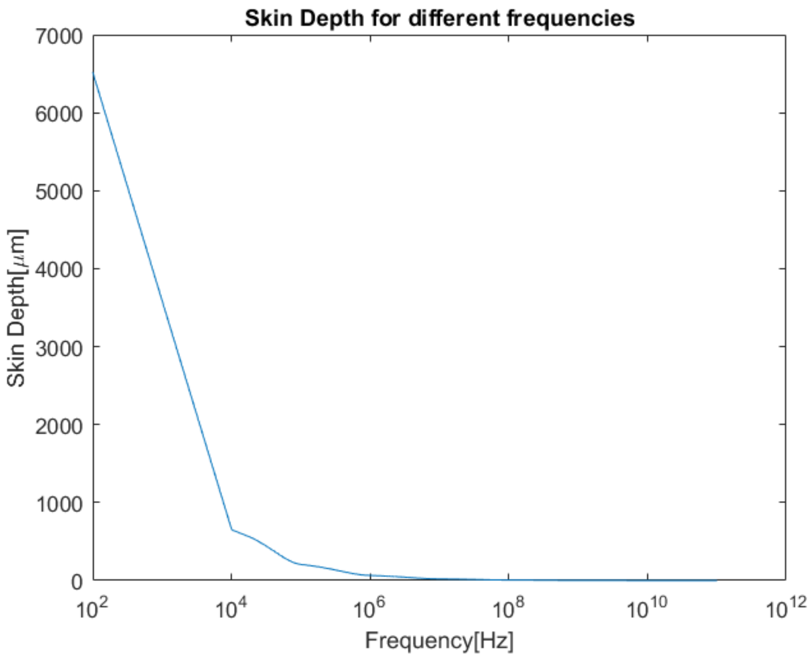

Figure 16.: *Frequency spectrum of the current waveform depicted in figure 14. The DC component of this signal was subtracted from the current pulse for better insight in low frequency components.*

Considering the frequency spectrum of the current pulse as shown in figure 15 we can conclude that skin effect is not a problem as the skin depth is much larger than the wire thickness which is between 0.5 mm and 1.5 mm. This is an advantage considering heating and force on the wire as will be discussed in section 9 and 10, respectively.

7.4 magnetic and induced electric fields

The intensity of the magnetic field and induced electric field in the head are dependent on the coil geometry. However, the waveform of these fields, as depicted in figure 17 and figure 18 are the same for all coils and only dependent on the current pulse. These fields were calculated 5 mm inside the head for the the figure-8 coil described in the next section.

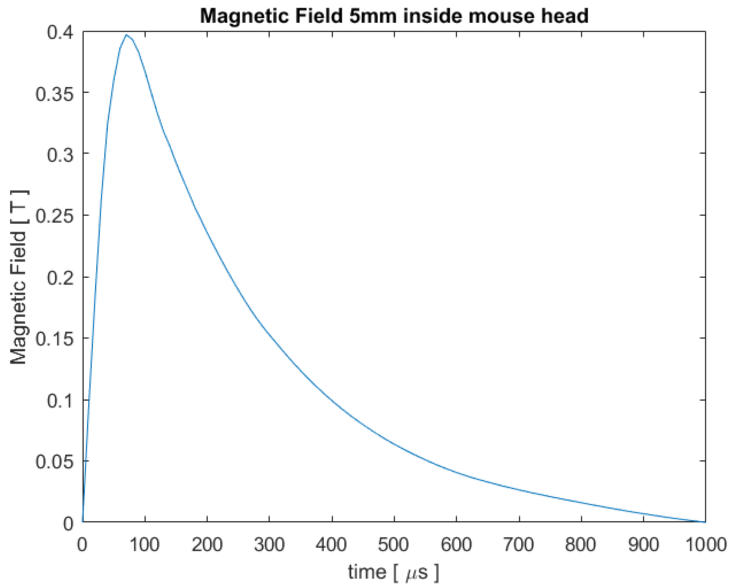

Figure 17.: *Magnetic field 5 mm inside mouse head model*

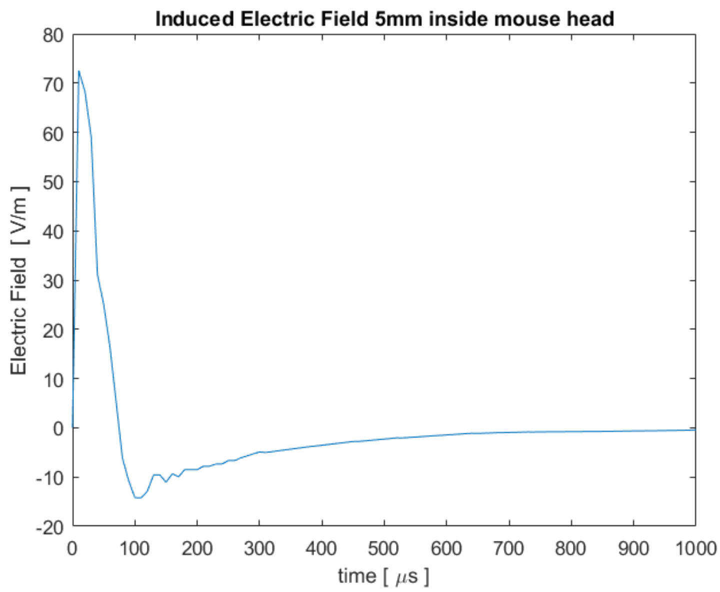

Figure 18.: *Electric field 5 mm inside mouse head model*

7.5 coil geometry comparison

We considered different coil configurations based on the figure-8 coil and analyze their performance parameters. All coils were driven by the same current, had seven turns of 1 mm thick wire, and an inner radius of 3 mm. Only the slinky coil has quite a different geometry compared to the rest as it has 32 turns spread out around its axis. The different models are depicted in figure 19. The intensity of the magnetic and induced electric field at a surface 5 mm inside the head are shown in appendix A.

For all these coils the performance parameters were calculated. The results are shown in table 2.

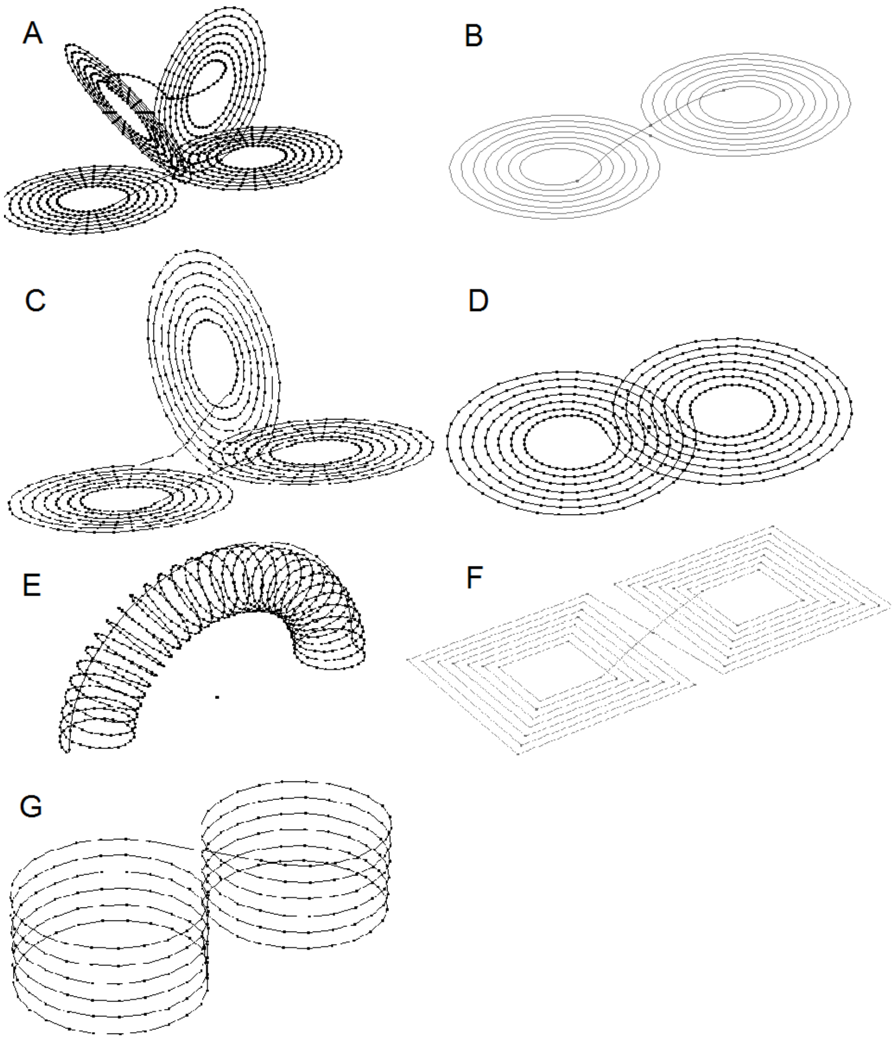

Figure 19.: *Models compared on focality and intensity performance parameters. A: Butterfly Coil. B: Figure-8 Coil. C: Orthogonal Figure-8 Coil. D: Overlap Figure-8 Coil. E: Slinky Coil. F: Square Figure-8 Coil. G: Binocular Figure-8 Coil.*

Table 2.: *Performance parameters for different models with 7 turns, inner radius of 3 mm and 1 mm wire thickness.*

Models	Figure 8	Butterfly	Overlap	Orthogonal	Square	Slinky	Binocular
Emax[V/m]	72.51	139.87	68.83	105.45	86.28	27.93	23.23
Half Value Volume [mm^3]	214.16	261.38	147.26	245.73	250.39	505.63	123.9
Half Value Depth [mm]	4.54	5.01	3.69	4.88	4.88	8.02	3.69
Focality [mm^2]	47.20	52.13	39.92	50.32	51.31	63.03	33.56

From these results it becomes clear that the binocular figure-8 coil is the best in terms of focality. However, the induced electric field intensity set by the requirements is not met. As more layers are added, the distance to the aspired stimulation point increases. Because of this distance, extra layers have no significant influence on the magnetic field strength [33], and thus neither on the induced electric field. We can thus conclude that the figure-8 and overlap coils are most suited in terms of focality and intensity.

7.6 Influence of wire thickness and inner radius on performance parameters

Coil geometry parameters like wire thickness, inner radius and number of turns determine the magnetic field intensities and distributions inside the brain and thus the performance parameters. To analyze this influence, we calculated the performance parameters for a figure-8 coil with a 0.5 mm diameter wire and seven turns while varying the inner radius of the coil. This was also done for 1 mm and 1.5 mm, the results are depicted in figure 20.

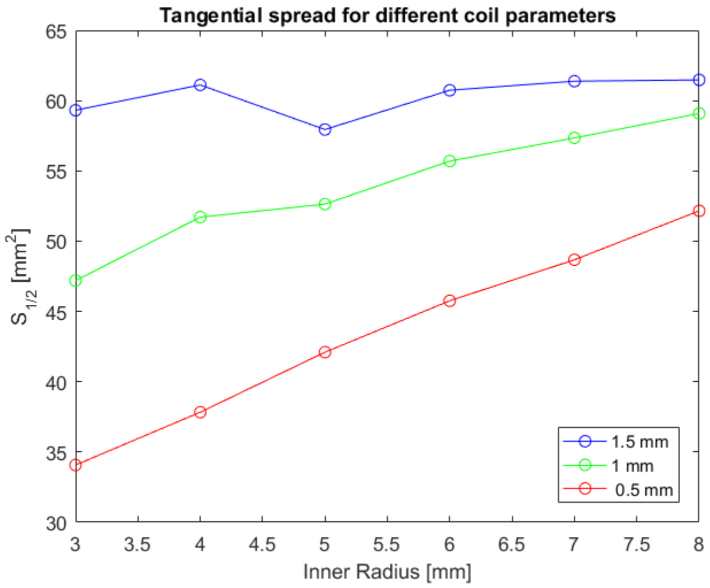

Figure 20.: *Calculated $S_{1/2}$ as a function of the coil inner radius for different wire diameters.*

The outer radius of the coil, as shown in figure 12, is dependent on the inner radius, number of turns and wire thickness, this relation becomes clear from equation 6.

$$R_{outer} = R_{inner} + (N_{turns} * Wire_{diameter}) \tag{6}$$

From these results it becomes clear that smaller figure-8 coils, with thinner wires and smaller inner radius are more focal. However, the induced electric field intensity decreases with thinner wires and smaller inner radius as illustrated in figure 21.

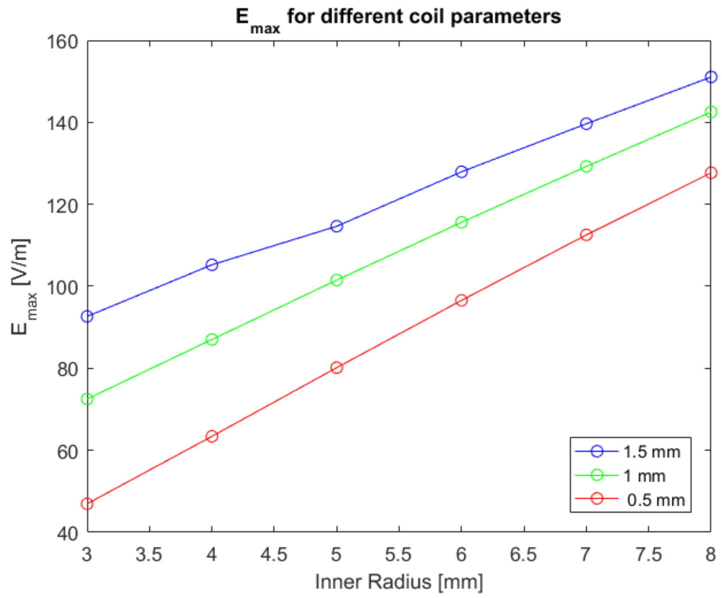

Figure 21.: *Calculated E_{max} as a function of the coil inner radius for different wire diameters.*

The ideal figure-8 coil would have thick wire to induce the necessary electric field intensity, but also be small enough to meet the focality criteria. However, it's not physically possible to make a figure-8 coil with 1.5 mm wire, and an inner and outer radius of 3mm and 10mm respectively. Therefore we must find the right balance between focality and intensity of the electric field.

7.7 INFLUENCE OF THE NUMBER OF TURNS ON PERFORMANCE PARAMETERS

The number of turns increases the magnetic field, and therefore has an effect on the intensity of the induced electric field. We studied this influence for a standard figure-8 coil by varying the number of windings and calculating the performance parameters. The inner and outer radius were left unchanged while varying the number of turns. The results are shown in table 3.

Table 3.: *Performance parameters for the figure-8 coil, with an inner radius of 3 mm and outer radius of 6 mm, with different number of windings.*

Turns	2 Turns	3 Turns	4 Turns	5 Turns	6 Turns	7 Turns	8 Turns
Emax$[V/m]$	11.58	17.942	24.38	30.24	36.56	42.70	49.78
Half Value Volume $[mm^3]$	94.59	98.128	97.27	98.14	98.86	100.19	98.54
Half Value Depth $[mm]$	3.07	2.94	2.93	3.09	3.05	3.03	3.07
Focality $[mm^2]$	30.81	33.40	33.22	31.78	32.47	33.11	32.14

7.8 final models

As mentioned in section 7.5 the two best models in terms of focality are the figure-8 coil and the figure-8 overlap coil. However, a higher electric field must be induced, so more turns must be added.
Here, these two models are analyzed for a different number of turns. Even though the results in figure 20 and 21 show that thinner wire leads to better forcality, 1 mm wire is used in these simulations due to heating and force issues explained in section 9 and 10. The inner radius is chosen to be 2 mm, because a smaller inner radius leads to better focality but it is not made smaller due to the inability to properly bend the wire. The results are shown in tables 4 and 5.

Table 4.: *Figure-8 coil performance parameters with 1 mm wire and inner radius of 2 mm.*

Number of turns	8	9	10	11
Emax [V/m]	74.122	91.36	109.77	128.84
Half Value Volume [mm^3]	241.86	250.26	281.69	319.12
Half-value depth [mm]	4.857	4.9	5.677	6.121
Focality [mm^2]	44.24	51.07	49.62	52.14

Table 5.: *Figure-8 overlap coil performance parameters with 1 mm wire and inner radius of 2 mm.*

Number of turns	8	9	10	11
Emax [V/m]	65.55	82.80	102.00	122.56
Half Value Volume [mm^3]	141.31	162.23	181.35	202.89
Half-value depth [mm]	3.91	4.21	4.47	4.718
Focality [mm^2]	36.18	38.53	40.60	43.00

8

WIRE CHOICE

To choose the right wire there are a couple of parameters to consider. Those are: electrical and thermal conductivity, flexibility, stiffness, and electrical insulation thickness. Copper is the standard wire for many applications as it has a higher electrical and thermal conductivity than nearly every other metal. Only silver does better in terms of these characteristics but is also a lot more expensive [34][35]. Higher electrical conductivity would lead to less heat generation while higher thermal conductivity leads to more dissipation of heat. Copper has a higher Young's modulus than silver, meaning that it's more stress resistant [36]. This could prove useful against forces generated inside the coil. Even though silver has a slightly higher electrical and thermal conductivity than copper, copper is cheaper and readily available and thus the preferred choice.

Lastly, insulation thickness and wire shape is important because tightly wound wire leads to a better magnetic field distribution.
Rectangle wire has shown to outperform round and square wires for smaller coils [33]. Therefore we decided to use rectangular copper magnet wire as it has a very thin layer of electrical insulation, and can be tightly wound.

9

HEATING

A primary concern with the development of small coils that have to handle such large currents is the inevitable heat generation. Considering that the coil casing is in contact with the mouse head, it's important that the heat dissipation is within safe limits for the mouse. As specified in the system requirements, the maximum allowed casing temperature is 41 °C.

Close temperature monitoring is therefore important. To achieve this we will place a MCP9700-E/TO temperature sensor [37] close to the coil. The sensor accuracy is sufficient at 1 °C which is the most important parameter.

The RMS value of the current (I_{rms}) as displayed in figure 14 is calculated via MATLAB to be 993 A. Via equation 7, the power dissipation (P) is calculated. It should be noted that this current is a worst case scenario with actual current flow until 1 ms. Depending on the final hardware it might very well be possible to have a shorter current flow duration. The coil resistance (R) varies per coil but is calculated as 24 mΩ for a coil with ten windings leading to a wire length of 106 cm with the wire having a 1 mm diameter. Because there is no skin effect at play, the effective resistance is not lowered.

$$P = I_{rms}^2 \cdot R \tag{7}$$

The result indicates 23.67 kW of power dissipation. Release of energy occurs only for a period of 1000 µs equaling 23.67 J (Q). The coil mass (m) can be calculated with the total wire volume and the volumetric mass density of copper: 8.94 $\mathrm{gcm^{-3}}$, equaling 28 gram. In combination with the specific heat of copper (c) equaling 0.386 $\mathrm{Jg^{-1}K^{-1}}$, the temperature increase (ΔT) can be found with equation 8.

$$Q = cm\Delta T \tag{8}$$

The temperature increase associated with one pulse is found to be 2.2 °C. Assuming an initial coil temperature of 25 °C, the coil can handle a maximum of seven consecutive pulses before the temperature limit of 41 °C is exceeded. It should be noted that the wire insulation is made out of polyurethane. The maximum heat handling capacity of this insulation is 150 °C, therefore the operating temperature of the coil will remain well below this limit.

According to general coil requirement 4, the lowest possible ISI is 1.5 ms. Coil requirement 5 states that paired pulses could follow each other up every five seconds. Therefore it has to become clear how much the coil cools down over time. There are three types of heat travel: conduction, convection and radiation. In this case convection is dominant because the heat transfer is from a solid (coil) to a fluid (air). This allows us to use equation 9, here Newton's law of cooling is referenced which can be used to calculate the cool down duration.

$$\Delta Q = hA(T(t) - T_{env}) \tag{9}$$

The total energy dissipated into air over time (ΔQ) is expressed as a function of the heat transfer coefficient (h), the surface area of the object (A), and the temperature difference between the object and the environment. The heat transfer coefficient for air varies greatly depending on the speed of the air. The casing will have vents on top to allow coil heat to escape into the air. Without active cooling we can assume a heat transfer coefficient of $5\,\mathrm{Wm^{-2}K^{-1}}$ [38]. The total surface area of the wire is $3.14 \times 10^{-3}\mathrm{m}^2$. As the wire and environment temperature are 41 °C and 25 °C respectively, the power dissipation equals 0.25 W. Because the released energy equals 23.67 J, it can be calculated that it takes about 95 seconds for the wire to cool back down to 25 °C.

It should be noted that this is merely the case for a single pulse. Paired pulse TMS utilizes two pulses meaning that double the amount of energy (47.34 J) is released. Using equation 8 it can be found that after a paired pulse the wire temperature has increased by 4.4 °C. The heat loss is recalculated with equation 9 as 70 mW at a temperature of 29.4 °C. This means that in the following five seconds only 0.35 J can be dissipated into the air, equaling a mere temperature drop of 0.03 °C. When the coil reaches 41 °C, the temperature after five seconds has fallen down a bit faster but still only by 0.1 °C. As there is virtually no cool down five seconds after a paired pulse the temperature rise will still amount to about 4.4 °C. Therefore three is the maximum amount of paired pulses allowed through the coil.

According to these calculations a coil without cooling would not comply to coil requirement 6. Thinner wire thus therefore not seem feasible. Practice will have to determine whether the heating concerns are legitimate. In case they are, cooling measures have to be explored. The objective is to increase the heat transfer coefficient because this leads to more heat transfer. An import factor is the velocity of air, higher velocities lead to higher heat transfer coefficients. One way to

achieve this is with the use of axial fans.
It is hard to determine an exact heat transfer coefficient so its effect will need to be studied once the whole system is complete. Two fan cooling concepts are considered for the coil. Option 1 would be to have two fans, one for each circular coil. Option 2 is one big fan for both circular coils. However, because axial fans are square while the coil casing's length is twice its width, not the complete fan capability would be used. Therefore option 1 is preferred, hereby two 30 mm × 30 mm fans as displayed in figure 22 will be ingrained next to each other in the coil casing. Disadvantages are the noise generated and the airflow that is caused which could startle the mouse.

Figure 22.: *A 30 mm x 30 mm fan to be used for coil cooling.*

Another option is water cooling which requires a water block, radiator, reservoir, pump, tubes and fans as seen in figure 23 [39]. It's an extensive system that might be hard to install and might limit coil manoeuvrability. However two advantages are a noiseless coil system and excellent cooling because of the relatively high thermal conductivity of water as opposed to air.

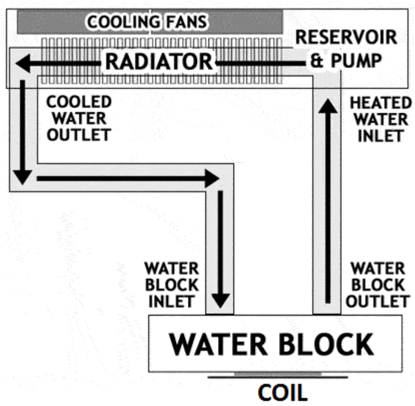

Figure 23.: *Water cooling setup for coil [39].*

A water block usually consists of metal which could influence the magnetic field, besides that it might be hard to find a water block in the right size. Therefore we consider removal of the water block and have the tubes go over the coil directly instead.

An unsuitable option is the heat sink. Heat sinks are simply not suitable because they are made out of metal.

If additional cooling is considered necessary, air cooling will be tried first. Even though the cooling capability might be worse than water cooling, if it proves to be sufficient while the noise is not an issue for the mouse, then it will be preferred because it's easier to install and has less components that might break down. In case air cooling is not sufficient, the fans necessary for water cooling are already available while the rest of the equipment can be ordered.

To see how heat influences the casing we set up a simulation. An actual test would have been ideal but was not possible yet because the required hardware was not available yet. Other equipment capable of delivering the current displayed in figure 14, or similar, to the coil was not within our reach either. Therefore the coil is simulated with a heat gun, while the 3D printed coil casing was available already. A limiting factor of the heat gun is that the minimum temperature is 50 °C and moves up with steps of 10 °C. Therefore the coil was simulated as having a temperature of 50 °C while not further increasing in temperature. The ambient and initial coil temperature were measured to be 24 °C and 26.1 °C, respectively. Figure 24 shows the casing's heating process. The upper left picture displays the starting condition whereby the coil is held steady by pliers. Subsequently the upper right picture shows the heat gun positioned behind the casing while it provides heat. The bottom pictures then show the cool down process whereby the heat gun is removed.

Figure 24.: *The upper left picture shows the initial coil temperature and experiment setup. The upper right picture shows the heat gun applied to the casing. The bottom pictures show the casing as it cools down.*

The heat simulation results are displayed in figure 25. As seen, the critical 41 °C temperature is reached after approximately 14 seconds. From there on it takes about 33 seconds for the casing to reach its maximum temperature of 49.2 °C. Subsequently the heat gun was removed and it can be seen that the temperature falls down exponentially. 114 seconds later the casing temperature was back to 29.6 °C. It can be observed that the rate of temperature drop depends on the casing temperature relative to the ambient temperature. As the casing temperature gets closer to the ambient temperature the rate of temperature decrease lessens. For example, five seconds after a casing temperature of 41 °C the temperature has dropped by 1 °C. However at a casing temperature of 32 °C the temperature has dropped by only 0.3 °C.

From this experiment we can observe that the casing will definitely absorb heat. It does take a while before the casing temperature would match the coil heat though. In this case it took about 23 seconds to reach 90% of the applied temperature, after which it took another 37 seconds to reach 98%. Short lasting coil temperature spikes above 41 °C should therefore not interfere with coil requirement 6. Another interesting note is that the casing started to deform as it reached 70 °C. To be within safe levels for the casing, the coil temperature should therefore never reach close or higher than 70 °C.

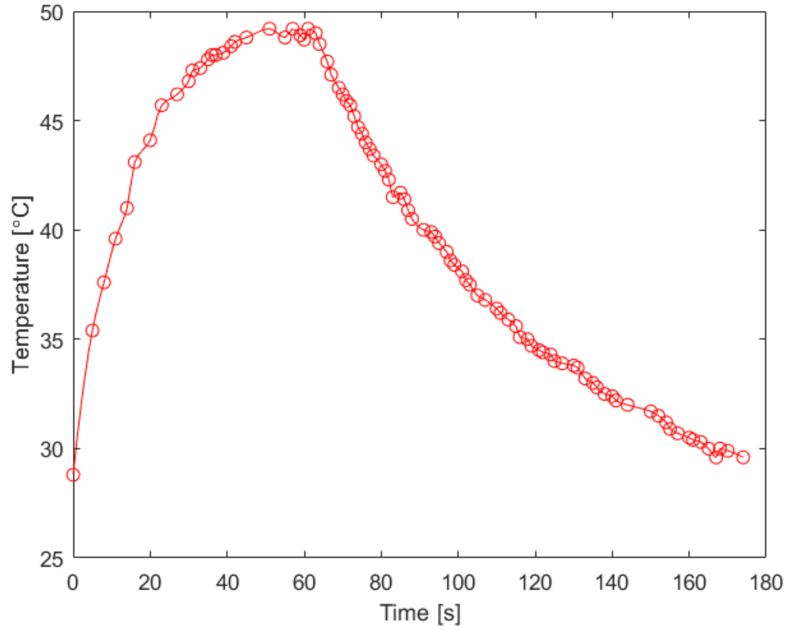

Figure 25.: *For about 65 seconds a heat gun provides a 50 °C airflow to the coil casing. Thereafter the heat gun is removed which causes the casing temperature to fall off exponentially.*

10

FORCE

TMS coils are bound to experience strong forces during operation. This is due to the magnetic field intensity and current flow through the coil. The Lorentz force density (**f**) shown in equation 10 is dependent on the current density (**J**) and the magnetic flux density (**B**).

$$\mathbf{f} = \mathbf{J} \times \mathbf{B} \tag{10}$$

The skin effect could influence the current density because current would be forced to flow through a smaller area leading to a higher current density. However as shown in 7.3, the skin effect is not of concern.

In COMSOL we modeled a circular coil in the 2D axisymmetric interface, figure 26 shows a plot of the cross section and the magnetic flux density. The corresponding Lorentz force density is shown in figure 27.

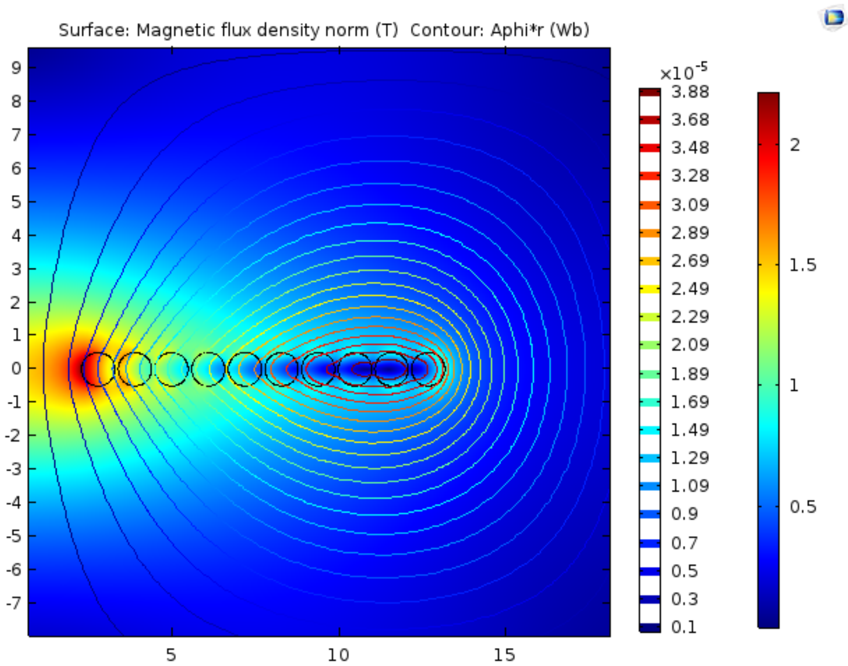

Figure 26.: *Magnetic flux distribution in the coil.*

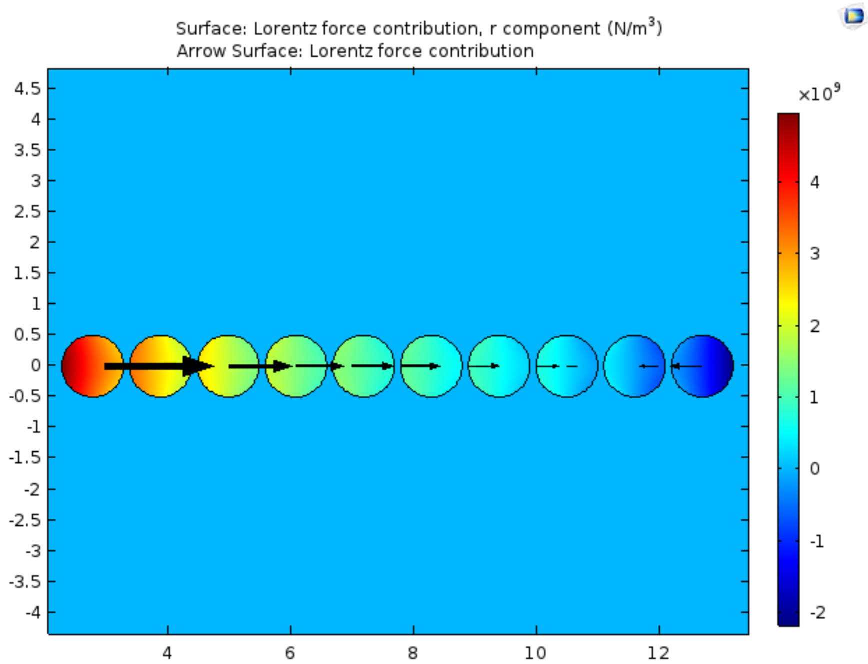

Figure 27.: *The Lorentz force causes the coil to compress itself on the outer side.*

It can be observed that the largest Lorentz force density is a bit higher than $4 \times 10^9\,\mathrm{Nm}^{-3}$. This is about $1 \times 10^9\,\mathrm{Nm}^{-3}$ higher than the force density value as reported in [40] which did not cause coil cracking. Therefore it's still unsure whether this force will cause big issues as it has not been tested.
As this is a circular coil model instead of a figure-8 model, caution has to be taken when considering these results. However this gives us a rough figure for the force and it appears that the coil is not to far off from force values that did not cause any issues.

Nonetheless, measures against the influence of force have to be taken as the wires are not allowed to move around. Therefore we will fill up the casing with epoxy to ensure the wires stay in place. The specific heat, indicating the amount of heat required to change a unit mass of substance by one degree in temperature [41], is virtually the same for air and epoxy. Whether epoxy will cause extra heating issues remains to be seen but it does not appear to be a big issue. Reality will have to show whether this solution is sufficient. If not, other measures such as thicker wire might be necessary as this leads to a lower current density.

11

COIL CHOICE

In the previous sections many calculations and considerations have been made. From Section 7 it has become clear that the figure-8 and overlap geometries have the highest focality. According to the results in figure 20, thin wire leads to better focality. Section 9 suggests that 1 mm wire might already lead to heating issues and thus thinner wire would not be favorable heating wise. A similar statement can be made about the force experienced. Section 10 states that the force experienced by the coil is right at a level the coil can still handle. We are not sure how much stronger the force may be before mechanical failure occurs. However via equation 10 it can be reasoned that because thinner wire would lead to a higher current density, the force experienced by the coil would increase. Therefore thinner wire is not desirable from a force perspective. Section 8 has indicated that copper wire is the best fit. Based on this analysis and the results shown in table 4 and table 5 we conclude that the most suitable coils are the figure-8 coil and the overlap coil with 1 mm copper wire, an inner radius of 2 mm, and each with 10 and 11 windings respectively. Additional measures such as epoxy are necessary to keep the wires in place, while (water) cooling might be necessary to ensure a safe operating temperature for repeated pulses.

12

INTERFACE WITH HARDWARE

As the coil draws current from the hardware this forms an interface. There are two ways to connect the coil to the hardware. Option 1 is to use connectors such that there is a connector on the coil and on the cable coming from the hardware. This would provide the benefit of having a detachable coil, allowing the use of different coils. However, suitable connectors are hard to find. Connectors usually have a specified (continuous) current limit, deriving the maximum current just for the short pulse the hardware sends is difficult. Connectors rated up to 1000 A which seem likely to work are usually scarce, large, and expensive. A possible solution might be the XT150 connector as shown in figure 28, with a rated current limit of 150 A, provide a low resistance and are steadily available.

Figure 28.: *The XT150 connector to detach the coil from hardware.*

Option 2 is to crimp the coil wire onto the hardware wire. This would not allow for detachability from the coil side. It could be possible to detach the wire on the hardware side meaning however that every coil would have a long wire attached to it. Crimping wires might provide a higher chance of operation than XT150 connectors as both wires are connected right onto each other without intervening equipment like a connector.

The first objective will be to use connectors. The coil wire should extend a bit more than usual so that the connector might be cut off in case of malfunctioning. In that case we move over to crimping.

13

COIL CASING

The TMS coil must be isolated from the environment to avoid electrical contact and burns. As this is the part of the system being most exposed to the patient and user, a proper coil container should be designed. Heating issues and the influence of the container materials on the magnetic and electric field distribution must be taken into account. In this chapter we discuss the design of the casing for the figure-8 coil to be build.

13.1 BUILD MATERIAL

The coil is designed to induce a specific magnetic field inside the head. The container should therefore have minimal influence on the magnetic field distribution. Most plastics have low relative permeability, which is a property suited for this application. For the creation of these containers we had 3D printers available that printed models out of polyactic acid (PLA).

PLA has a melting point between 150–160 °C, which is sufficient in this case considering the coil won't reach such temperatures.
It should be noted that PLA based products can not be exposed to high humidity and therefore must be stored properly.

A model of the figure-8 coil casing is depicted in figure 29a below. The base of the casing has prints on it that resemble the location of the wire. This allows us to wind the coil inside the casing by placing the wire in these prints. The 3D printed casing for the figure-8 coil is illustrated in figure 29b.

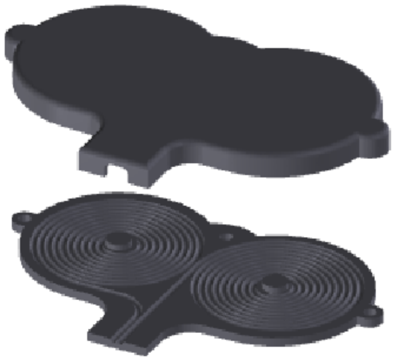

(a) *Casing Model*

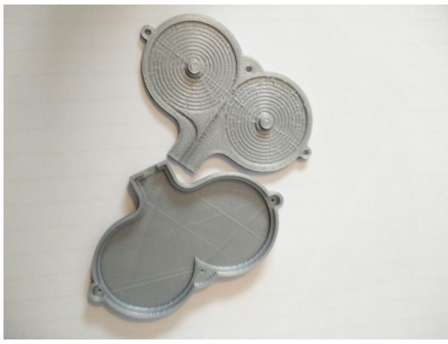

(b) *3D Printed casing*

Figure 29.: *Figure-8 coil casing*

This model will be used to test coil heating without any external cooling. Casing for the figure-8 coil with fans and the overlap figure-8 coil are still being designed.
Another potential material is Acrylonitrile Butadiene Styrene (ABS). Benefits of ABS over PLA are the higher melting point and stiffness. Therefore this material might be better suited for this application. For us printing with ABS however was less accessible but might be possible in the future. Therefore PLA was the first option but we are now looking at using ABS.

14

DISCUSSION

In this chapter we will reflect on the specifications given in Section 6.

Below table 1 is displayed supplemented with a check mark indicating whether the requirement is theoretically met or not.

Nr.	Requirement	Requirement/Wish	$\surd$/X
1	All system components in contact with user and patient should be electrically isolated	Requirement	$\surd$
2	The coil should have a suitable casing	Requirement	$\surd$
3	The coil should be able to handle paired pulses with interstimilus interval (ISI) of 3 ms	Requirement	$\surd$
4	The coil should be able to handle paired pulses with an interstimulus interval (ISI) programmable between 1.5 ms and 3 ms	Wish	$\surd$
5	The coil should be able to handle a paired pulse followed by another paired pulse five seconds later repetitively for 200 times.	Requirement	?
6	The casing should be kept at a temperature lower than 41 °C at the surface in contact with the mouse head	Requirement	?
7	The induced electric field should be at least $110\,\mathrm{V\,m^{-1}}$, 5 mm deep in the head	Requirement	$\surd$
8	The electric field should stimulate a maximum area of 1 mm x 1 mm	Requirement	-
9	The electric field should stimulate a maximum area of 0.5 mm x 0.5 mm	Wish	-
10	The designed coil must be a figure-8 coil	Requirement	$\surd$
11	Alternative coil geometries derived from the figure-8 coil may be designed as well	Wish	$\surd$

Requirement 1 and 2 are met because the coil wire is electrically isolated and encapsulated in a casing made out of PLA. Requirement 3 up to and including 6 are met, as in the case of heating issues, active cooling can be employed. According to simulations, the induced electric field will be at least $110\,\mathrm{Vm}^{-1}$ or higher as specified by requirement 7. As mentioned earlier, requirement 8 and 9 are not uniquely defined and are therefore hard to comply with. We have set out to increase focality compared to existing TMS coils. In that regard we have succeeded. The two proposed coils are an actual and derived figure-8 coil respectively, therefore requirements 10 and 11 are met.

Theoretically the answer to the problem stated in Section 3 can be answered with *yes*. A dark horse might be force exerted on the coil as it is not exactly clear what influence certain magnitudes have. Therefore reality will have to confirm this answer.

Part III

TESTPLAN

14.1 TEST PLAN

To verify the workings and safety of our product we will first put it through testing. Unfortunately at time of writing it's not yet possible to test coils because the required hard- and software is not available yet, therefore we will describe our proposed test plan.

The first step will be to put a low current pulse through the coil. Depending on the hardware capability we will start off with the lowest possible current, and gradually turn up the current until we reach the specified 2.5 kA. If the coil does not show any signs of tear down or damage we can start measuring important parameters. These parameters are the magnetic field strength, heat generation, run time, and durability. The following sections will describe how we plan on doing that.

14.1.1 *Magnetic field strength*

The objective is to measure the magnetic field and compare it to the simulated magnetic field. If the measured and simulated fields are approximately the same we can infer the simulations are correct and that the simulated electric field should translate to reality as well. Hall probes provide an easy way of measuring the magnetic field, ideally they can be connected to a computer so all data can be read out and stored.

14.1.2 *Heat and run time*

Heat production will be measured by the temperature sensor build into the coil casing. The coil will first receive a single pulse to observe the heat generated. In case this is in accordance to our calculations or lower, a paired pulse can be sent and the same procedure will apply. Hereafter its possible to check how many paired pulse with five second period in between can be send before the temperature reaches 41 °C. Ideally this is possible for at least 200 consecutive pulses.
If this is not the case, the fans described in Section 9 will have to be installed. Subsequently the maximum amount of pulses before reaching 41 °C will have to be recorded again. If hereafter heating would still be an issue, we might have to look into using thicker wire, this would be at the expense of focality.

14.1.3 *Durability*

If previous tests have gone well it's possible to test the coil's durability. This would mean sending 200 consecutive pulses through the coil where after we wait until the coil reaches its initial temperature again.

Subsequently another batch of pulses can be sent, this process should be repeated at least twenty times to see whether the coil is suitable for prolonged use.

Part IV

FINAL THOUGHTS

15

COMPARISON OF OUR MODEL WITH EXISTING COILS

With the focality parameter $S_{1/2}$ we can now objectively compare our design to existing coils. Figure 30 displays the focality of different coils compared to our own design.

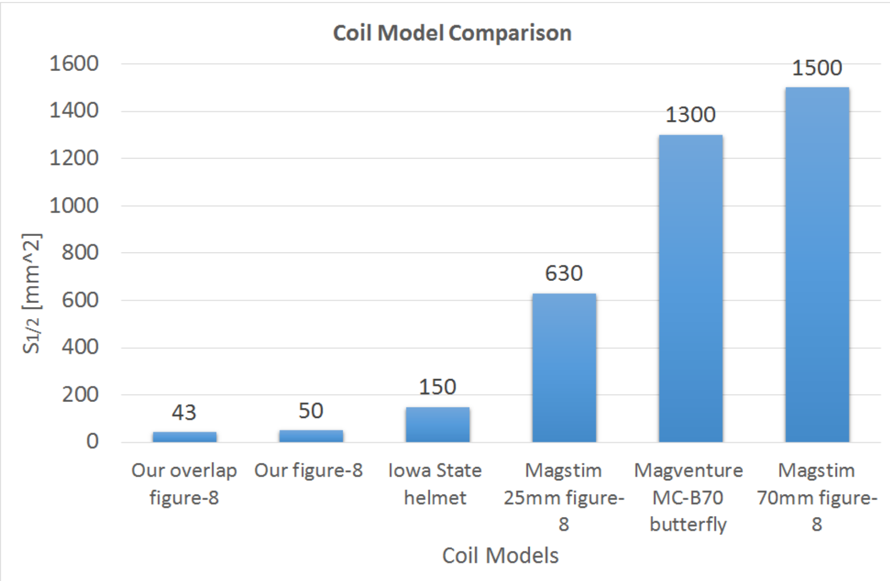

Figure 30.: *Comparison of different TMS coils in terms of focality defined by the tangential spread $S_{1/2}$ in mm^2.*

It should be noted that except for the Iowa State helmet coil, all of these coils are designed for the human specimen. Nonetheless we can observe that the value of our focality is much lower as compared to the rest, indicating that a smaller brain region is stimulated. Even compared to the design of the Iowa State University coil for mice we have realized a focality about three times better. As mentioned in Section 6, coil requirement 8 indicating a focality of 1 mm^2 is loosely defined but we can conclude that we have reached the best focality of TMS coils thus far.

16

CONCLUSION

In about two months time we have set up the foundation for the realisation of a focal TMS coil suitable for mice. The focality we have reached is better than that of existing coils. The theoretical design takes focality, heating, packaging and forces into account and adheres to the requirements set in the system specifications. A path to the practical realisation of the coil has been set. The possibility to carry out tests is dependent on the realisation of the developed hardware and software. Once the remaining equipment is realized, the coil can be tested according to the test plan we have set up.

We thoroughly enjoyed the opportunity to apply our accumulated knowledge throughout the years in a team setting to realize a product. We hope that the hardware, software and coil combine into a solid product capable of performing Transcranial Magnetic Stimulation on mice. Furthermore we hope to have excited the reader for TMS and hope they can benefit from the theoretical framework that has been set.

BIBLIOGRAPHY

[1] M. Kobayashi and A. Pascual-Leone, "Transcranial magnetic stimulation in neurology," *THE LANCET Neurology*, vol. 2, no. 3, pp. 145–156, 2003.

[2] J. C. Horvath, J. Mathews, M. A. Demitrack, and A. Pascual-Leone, "The neurostar tms device: Conducting the fda approved protocol for treatment of depression," *Journal of Visualized Experiments*, vol. 45, 2010.

[3] J. C. Horvath, J. M. Perez, L. Forrow, F. Fregni, and A. Pascual-Leone, "Transcranial magnetic stimulation: a historical evaluation and future prognosis of therapeutically relevant ethical concerns," *J Med Ethics*, vol. 37, pp. 137–143, 2011.

[4] Z. J. Daskalakis, B. K. Christensen, P. B. Fitzgerald, and R. Chen, "Transcranial magnetic stimulation: A new investigational and treatment tool in psychiatry," *The Journal of Neuropsychiatry and Clinical Neurosciences*, vol. 14, no. 4, pp. 406–415, 2002.

[5] B. Basil, J. Mahmud, and B. Adetunji, "Is there evidence for effectiveness of transcranial magnetic stimulation in the treatment of psychiatric disorders?" *Psychiatry (Edgmont)*, vol. 2, no. 11, p. 64–69, 2004.

[6] E. M. Wassermann and T. Zimmermann, "Transcranial magnetic brain stimulation: Therapeutic promises and scientific gaps," *Pharmacology & Theurapeutics*, vol. 133, no. 1, pp. 98–107, 2012.

[7] K. A. Zimmermann, "Nervous system: Facts, function & diseases," 2016. [Online]. Available: http://www.livescience.com/22665-nervous-system.html

[8] B. Voytek. Are there really as many neurons in the human brain as stars in the milky way? [Online]. Available: http://www.nature.com/scitable/blog/brain-metrics/are_there_really_as_many

[9] J. H. Byrne. Introduction to neurons and neuronal networks. [Online]. Available: http://neuroscience.uth.tmc.edu/s1/introduction.html

[10] "Action potential." [Online]. Available: https://en.wikipedia.org/wiki/Action_potential

[11] F. T. Ulaby, E. Michielssen, and U. Ravaioli, *Fundamentals of Applied Electromagnetics 6e*. Prentice Hall, 2001.

[12] Using ampere's law. [Online]. Available: http://bulldog2.redlands.edu/facultyfolder/eric_hill/Phys332/Lectures/Day%2019.pdf

[13] Ampère's law and differential operators. [Online]. Available: http://www.physics.byu.edu/faculty/rees/220/book/Lesson8.pdf

[14] C. Furse, D. A. Christensen, and C. H. Durney, *Basic introduction to bioelectromagnetics*. CRC press, 2009.

[15] J. Larsson, "Electromagnetics from a quasistatic perspective," *American Journal of Physics*, vol. 75, no. 3, pp. 230–239, 2007.

[16] S. Rossia, M. Hallett, P. M. Rossinic, and A. Pascual-Leonee, "Safety, ethical considerations, and application guidelines for the use of transcranial magnetic stimulation in clinical practice and research," *Cinical Neurophysiology*, vol. 120, no. 12, pp. 2008–2039, 2009.

[17] F. Fujita and Y. Koga, "Clinical application of single-pulse transcranial magnetic stimulation for the treatment of depression," *Psychiatry and Clinical Neurosciences*, vol. 59, no. 4, pp. 425–432, 2005.

[18] N. Arai, S. Okabe, T. Furubayashi, Y. Terao, K. Yuasa, and Y. Ugawa, "Comparison between short train, monophasic and biphasic repetitive transcranial magnetic stimulation (rtms) of the human motor cortex," *Cinical Neurophysiology*, vol. 116, no. 3, pp. 605–613, 2004.

[19] E. M. Wassermann, "Side effects of repetitive magnetic stimulation," *The oficial journal of ADAA*, vol. 12, no. 3, pp. 124–129, 2000.

[20] I. F. A. T. Barker, R. Jalinous, "Non-invasive magnetic stimulation of human motor cortex," *The Lancet*, vol. 325, no. 8437, pp. 1106–1107, 1985.

[21] The birth of transcranial magnetic stimulation. [Online]. Available: http://www.magstim.com/heritage

[22] A. Thielscher and T. Kammer, "Electric field properties of two commercial figure-8 coils in tms: calculation of focality and efficiency," *Clinical neurophysiology*, vol. 115, no. 7, pp. 1697–1708, 2004.

[23] M. A. Abdeen and M. A. Stuchly, "Modeling of magnetic field stimulation of bent neurons," *Biomedical Engineering, IEEE Transactions On*, vol. 41, no. 11, pp. 1092–1095, 1994.

[24] Z.-D. Deng, S. H. Lisanby, and A. V. Peterchev, "Electric field depthefocality tradeoff in transcranial magnetic stimulation: Simulation comparison of 50 coil designs," *Brain Stimulation*, vol. 6, no. 1, pp. 1–13, 2013.

[25] Cool-40 rat coil. [Online]. Available: http://www.magventure.com/en-gb/Products/MagPro-coils/Special-Coils/Cool-40-Rat-Coil

[26] Body and brain weights. [Online]. Available: http://mste.illinois.edu/malcz/DATA/BIOLOGY/Animals.html

[27] S. D. March, S. J. Stark, R. L. Hadimani, D. R. Stiner, M. J. Senter, K. K. Spoth, L. J. Crowther, and D. C. Jiles, "Thermal and mechanical analysis of novel transcranial magnetic stimulation coil for mice," *Magnetics, IEEE Transactions on*, vol. 50, no. 9, pp. 1–5, 2014.

[28] L. J. Crowther, R. L. Hadimani, A. G. Kanthasamy, and D. C. Jiles, "Transcranial magnetic stimulation of mouse brain using high-resolution anatomical models," *Journal of Applied Physics*, vol. 115, no. 17, p. 17B303, 2014.

[29] P. Maccabee, V. Amassian, L. Eberle, and R. Cracco, "Magnetic coil stimulation of straight and bent amphibian and mammalian peripheral nerve in vitro: locus of excitation." *The Journal of Physiology*, vol. 460, p. 201, 1993.

[30] E. Allebes and T. Steunebrink, "Transcraniële magnetische stimulatie hardware en mechanisch ontwerp," 2016.

[31] A. N. Jahfari and E. Eland, "Transcraniële magnetische stimulator voor muizen: Softwareontwerp," 2016.

[32] H. Eaton, "Electric field induced in a spherical volume conductor from arbitrary coils: application to magnetic stimulation and meg," *Medical and Biological Engineering and Computing*, vol. 30, no. 4, pp. 433–440, 1992. [Online]. Available: http://dx.doi.org/10.1007/BF02446182

[33] M. Talebinejad and S. Musallam, "Effects of tms coil geometry on stimulation specificity," in *Engineering in Medicine and Biology Society (EMBC), 2010 Annual International Conference of the IEEE*. IEEE, 2010, pp. 1507–1510.

[34] Electrical conductivity in metals. [Online]. Available: http://metals.about.com/od/properties/a/Electrical-Conductivity-In-Metals.htm

[35] Thermal conductivity. [Online]. Available: http://hyperphysics.phy-astr.gsu.edu/hbase/tables/thrcn.html

[36] Young's modulus - tensile modulus or modulus of elasticity - for steel, glass, wood and other common materials. [Online]. Available: http://www.engineeringtoolbox.com/young-modulus-d_417.html

[37] *Low-Power Linear Active Thermistor ICs*, Microchip, 6 2016, rev. G. [Online]. Available: http://ww1.microchip.com/downloads/en/DeviceDoc/20001942G.pdf

[38] Convective heat transfer coefficients table chart. [Online]. Available: http://www.engineersedge.com/heat_transfer/convective_heat_transfer_coefficients__13378.htm

[39] D. Murphy. (2013) Liquid cooling vs. traditional cooling: What you need to know. [Online]. Available: http://www.pcworld.com/article/2028293/liquid-cooling-vs-traditional-cooling-what-you-need-to-know.html

[40] L. J. Crowther, K. Porzig, R. L. Hadimani, H. Brauer, and D. C. Jiles, "Realistically modeled transcranial magnetic stimulation coils for lorentz force and stress calculations during mri," *Magnetics, IEEE Transactions on*, vol. 49, no. 7, pp. 3426–3429, 2013.

[41] Specific heat of common substances. [Online]. Available: http://www.engineeringtoolbox.com/specific-heat-capacity-d_391.html

Part V

APPENDIX

A

MAGNETIC AND INDUCED ELECTRIC FIELD FOR DIFFERENT MODELS

In this appendix, we illustrate the magnetic and induced electric field 5 mm inside the head for the different coil models. The illustration aims to give better understanding of distribution of the fields inside the head. These results were calculated 10 µs into the current pulse described in Section 7.2.

A.1 BUTTERFLY COIL

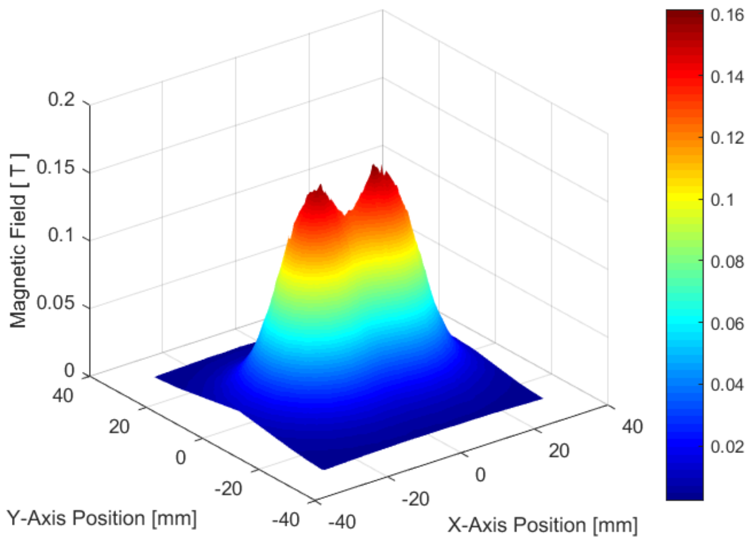

Figure 31.: *Magnetic field 5mm inside the head by the Butterfly Coil*

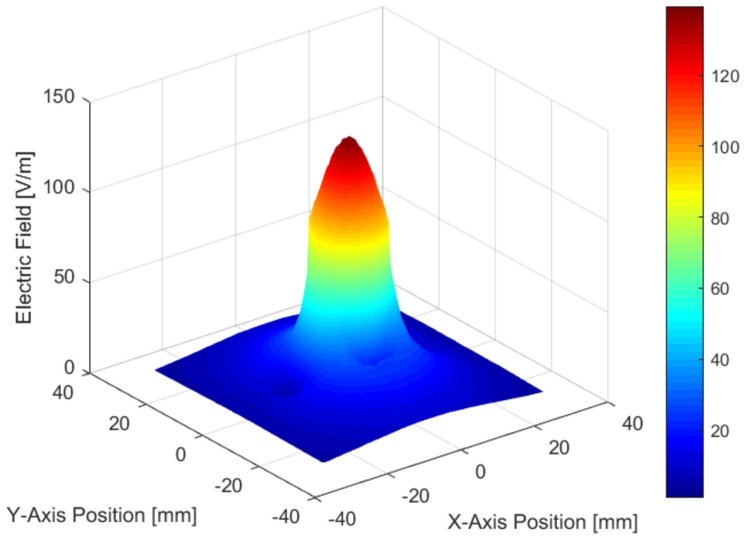

Figure 32.: *Induced electric field 5mm inside the head by the Butterfly Coil*

A.2 FIGURE-8 COIL

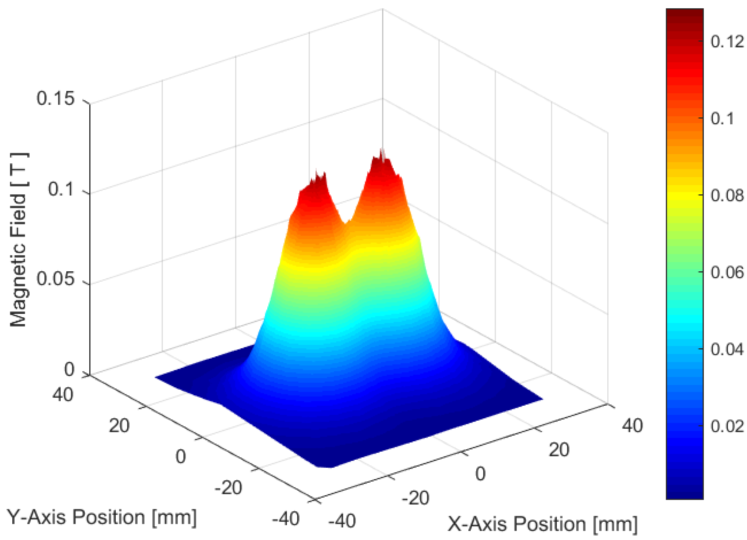

Figure 33.: *Magnetic field 5mm inside the head by the Figure-8 Coil*

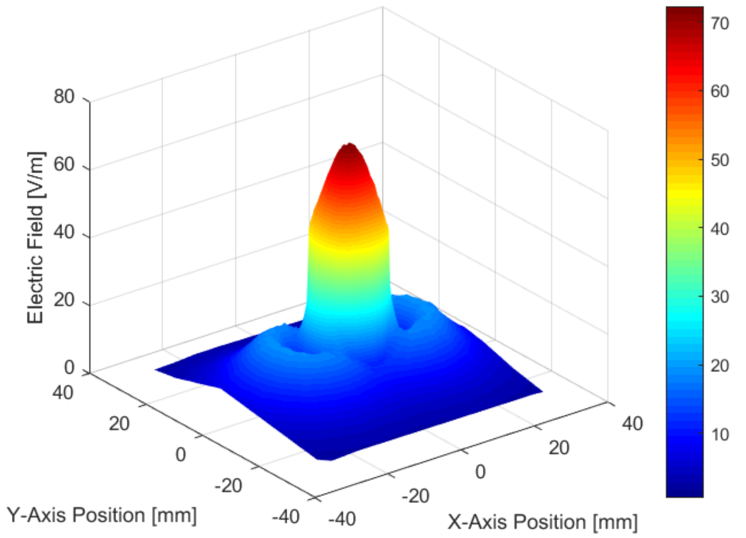

Figure 34.: *Induced electric field 5mm inside the head by the Figure-8 Coil*

A.3 ORTHOGONAL FIGURE-8 COIL

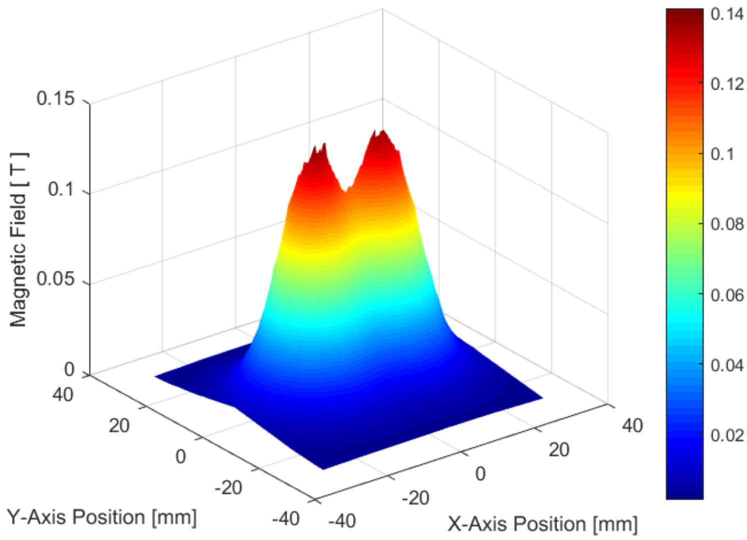

Figure 35.: *Magnetic field 5mm inside the head by the Orthogonal Figure-8 Coil*

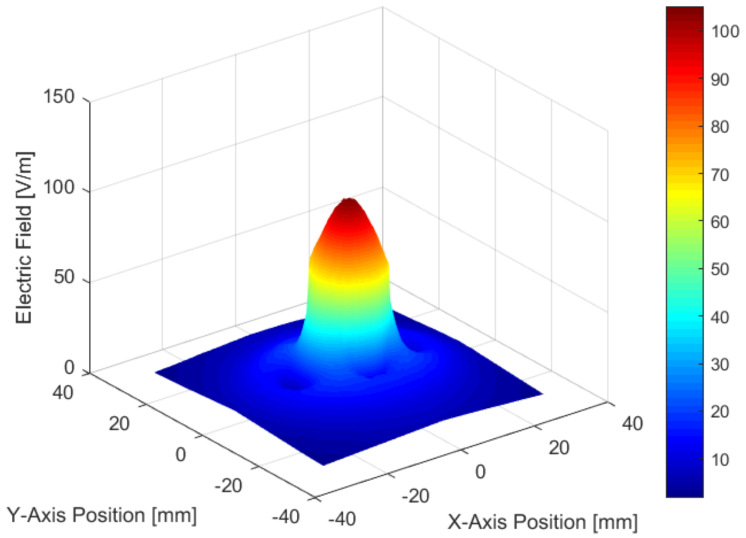

Figure 36.: *Induced electric field 5mm inside the head by the Orthogonal Figure-8 Coil*

A.4 OVERLAP FIGURE-8 COIL

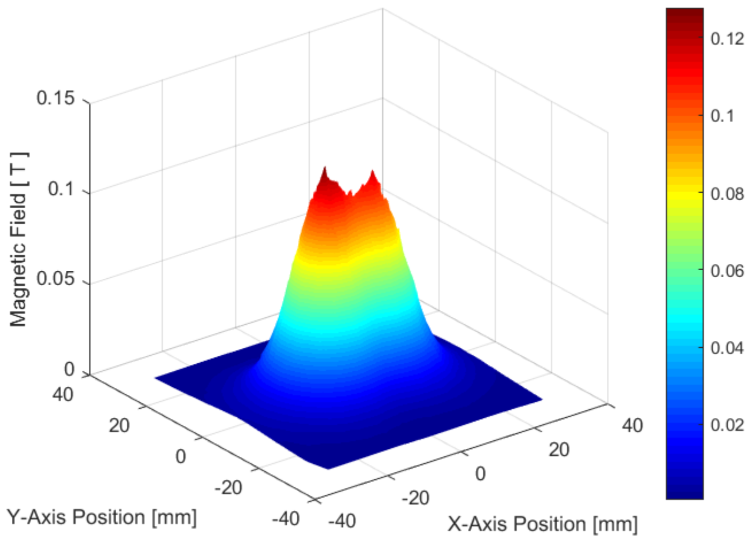

Figure 37.: *Magnetic field 5mm inside the head by the Overlap Figure-8 Coil*

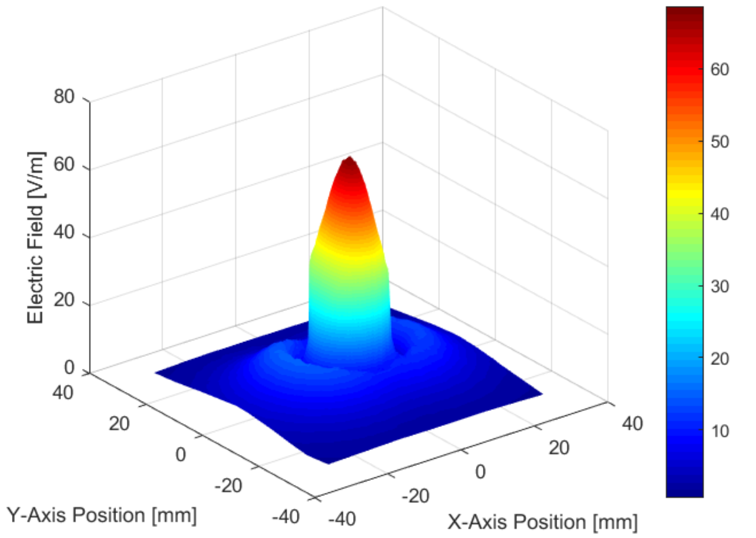

Figure 38.: *Induced electric field 5mm inside the head by the Overlap Figure-8 Coil*

A.5 SLINKY COIL

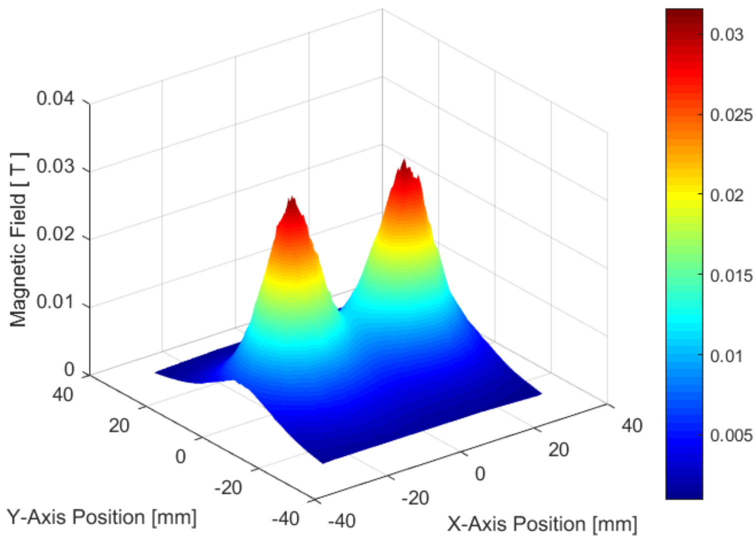

Figure 39.: *Magnetic field 5mm inside the head by the Slinky Coil*

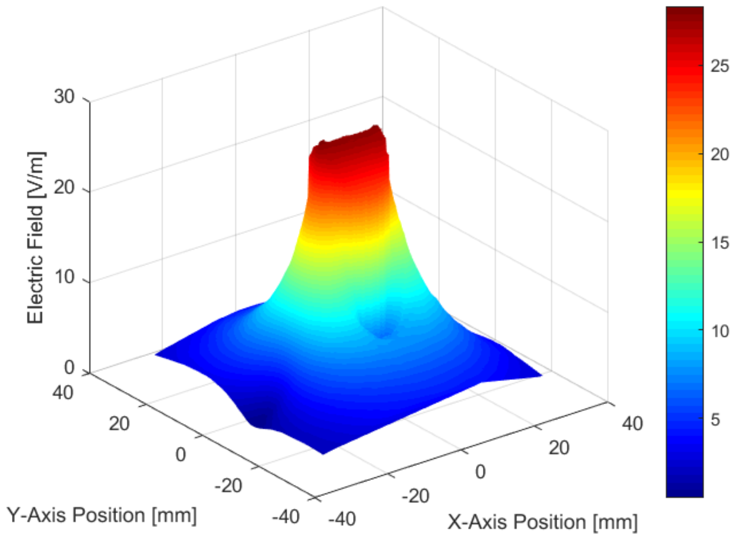

Figure 40.: *Induced electric field 5mm inside the head by the Slinky Coil*

A.6 SQUARE FIGURE-8 COIL

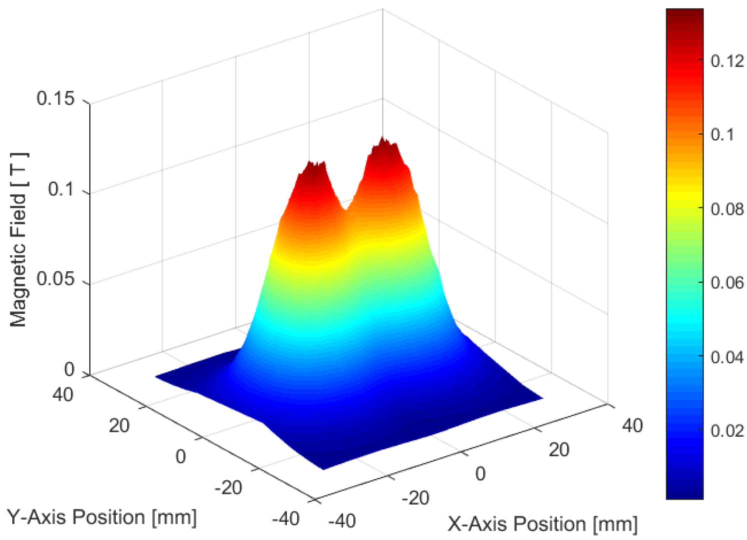

Figure 41.: *Magnetic field 5mm inside the head by the Square Figure-8 Coil*

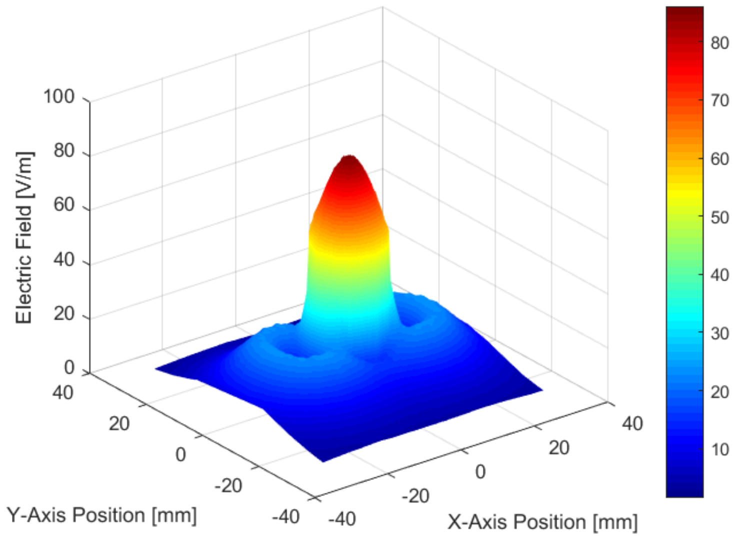

Figure 42.: *Induced electric field 5mm inside the head by the Square Figure-8 Coil*

A.7 BINOCULAR FIGURE-8 COIL

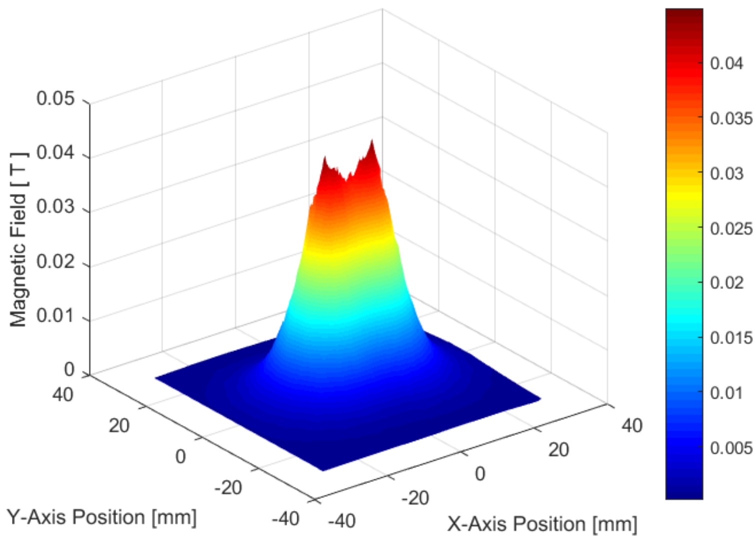

Figure 43.: *Magnetic field 5mm inside the head by the Binocular Figure-8 Coil*

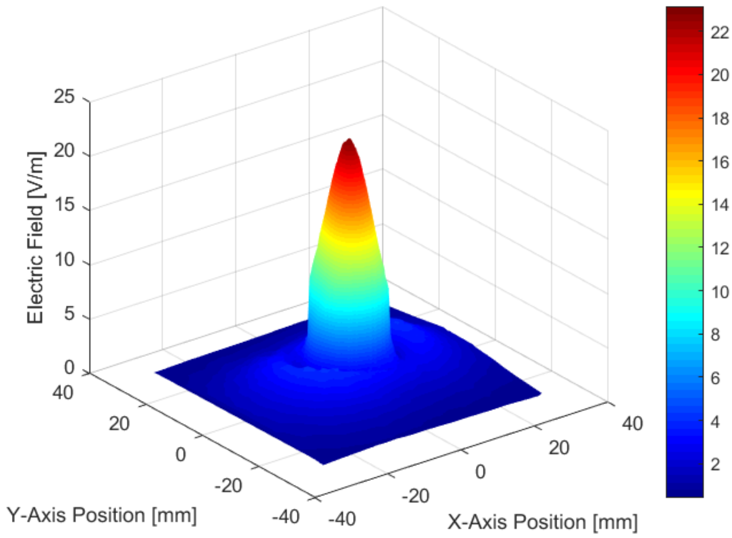

Figure 44.: *Induced electric field 5mm inside the head by the Binocular Figure-8 Coil*